Trends in Analytical Chemistry 109 (2018) 260–274

Contents lists available at ScienceDirect

Trends in Analytical Chemistry

journal homepage: www.elsevier.com/locate/trac

Recent advances in sensors for tetracycline antibiotics and their applications

Xigui Liu [a, b], Danlian Huang [a, b, *], Cui Lai [a, b, **], Guangming Zeng [a, b], Lei Qin [a, b], Chen Zhang [a, b], Huan Yi [a, b], Bisheng Li [a, b], Rui Deng [a, b], Shiyu Liu [a, b], Yujin Zhang [a, b]

[a] College of Environmental Science and Engineering, Hunan University, Changsha, Hunan 410082, China
[b] Key Laboratory of Environmental Biology and Pollution Control (Hunan University), Ministry of Education, Changsha, Hunan 410082, China

ARTICLE INFO

Article history:
Available online 19 October 2018

Keywords:
Tetracycline antibiotics
Human safety
Optical sensor
Electrochemical sensor
Quantitative detection

ABSTRACT

To control food safety, protect human safety and health, sensors for tetracycline antibiotics with easy operation, in-situ applications, high sensitivity and selectivity have been urgently needed. In this review, we provide an overview of recent advances and new trends in sensors for the detection of tetracycline antibiotics based on optical sensors, electrochemical sensors and other sensors including electrochemiluminescence and photoelectrochemical strategy. And we pay more attention to the practical applications of sensors for tetracycline antibiotics. Furthermore, a brief summary of the entire review, compare detection methods for different applications in the area of quantitative detection of tetracycline antibiotics, along with discussing the drawbacks of present sensors are concluded. Finally, the current challenges, ongoing efforts and future prospects in this field are also included to provide an overview for future research directions.

1. Introduction

Since their first introduction into medicine in the 1940s, antibiotics have been widely used in livestock farming and healthcare throughout the world [1–3]. Tetracycline antibiotics (TCs), as one kind of important broad-spectrum antibiotics [4,5], have been widely applied to human and animal medicine and foodstuff owing to the superior performance of effective antimicrobial properties, low-cost, and capability to improve growth rates and enhance feed efficiency [6]. Accurately, TCs can be divided into four main types: tetracycline (TC), oxytetracycline (OTC), chlortetracycline (CTC) and doxycycline (DC) [7]. Nevertheless, TCs are able to be accumulated in human body by food chain, which may result in pernicious effect on the human health even at low doses, like toxicity to organs and hearing loss [8,9]. Additionally, the abuse of TCs has improved the frequency of resistance genes, which may lead to a decrease in the efficiency of bacterial infections treatment [10,11]. Furthermore, the emergence of antibiotic-resistant bacteria is likely to spread to other microbial populations [12,13], triggering a potential negative effect to human and animal health [14,15]. Accordingly, the European Union (EU) had established maximum residue limits (MRLs) for milk (0.1 mg kg^{-1}), egg (0.2 mg kg^{-1}), liver (0.3 mg kg^{-1}) and kidney (0.6 mg kg^{-1}) samples [16], and the U.S. Food and Drug Administration (FDA) had set the MRLs for milk (0.4 mg kg^{-1}), fat (12 mg kg^{-1}), liver (6 mg kg^{-1}), and muscle (2 mg kg^{-1}) samples [17] to control the levels of TCs satisfying the security value. Hence, highly accurate, sensitive and selective detection methods for monitoring of TCs in food, serum and water are demanded to protect human safety and health [18,19].

In the past decades, numerous analytical methods have been developed for quantitative determination of TCs. Chromatographic methods including liquid chromatography-mass spectrometric (LC-MS) [7], high-performance liquid chromatography (HPLC) [20], and thin-layer chromatography (TLC) [21], are the most conventional detection methods for TCs. However, some inherent disadvantages of chromatographic methods, such as the time-consuming, professional operation skill, and expensive apparatus have limited their widely applications. Except chromatographic methods, capillary electrophoresis (CE) [22], capillary electrophoresis-mass spectrometric (CE-MS) [23], and enzyme-linked immunosorbent assay (ELISA) [24], are also successfully established for the

* Corresponding author. College of Environmental Science and Engineering, Hunan University, Changsha 410082, PR China.
** Corresponding author. College of Environmental Science and Engineering, Hunan University, Changsha, Hunan 410082, China.
E-mail addresses: huangdanlian@hnu.edu.cn (D. Huang), laicui@hnu.edu.cn (C. Lai).

https://doi.org/10.1016/j.trac.2018.10.011
0165-9936/

detection of TCs with highly sensitivity and accuracy, but still exist some drawbacks such as complicate sample pretreatment process and requirement of highly trained technical personnel [25]. Therefore, a group of simple, convenient, robust, and rapid but also sensitive, and selective detection methods for TCs are highly demanded.

Great efforts have been devoted to exploring alternative strategies for sensing of TCs in a facile, rapid, selective, sensitive, user-friendly and accurate manner [26]. Sensors emerge as promising, innovative, and complementary or alternative analytical techniques for the detection of antibiotics because of their superiorities of high sensitivity and selectivity, rapid detection, easy operation, and in-situ applications [27–29]. Therefore, a significant attention has been drawn to the fabrication of sensors for TCs detection. Vast sensing strategies such as optical-based sensors, electrochemical-based sensors and other sensors including electrochemiluminescence-based sensor and photoelectrochemical-based sensor, have been established for TCs analysis [25,27,30–34]. Those sensors utilizing recognition elements ((bio)receptors) such as aptamer, enzyme, molecularly-imprinted polymers, small molecular and macromolecule chemicals, and antibody etc., which can be employed to directly identify and capture the target TCs [25,33,35–37]. Moreover, different kinds of nanomaterials such as gold nanoparticles [38,39], graphene [40,41], magnetic nanoparticles [42,43], carbon dots [44,45] and quantum dots [46,47], etc. have been applied to construct those TCs sensors. The integration of nanomaterials and recognition elements shows excellent selectivity and high sensitivity in terms of real-time analysis, which is in high demand for TCs detection [30,34].

In the last few years, there is a rapid increase in fabrication of antibiotics sensors. For example, a review about the biosensors for the detection of antibiotics was reported by Lan et al. [25], Robati and co-workers summarized a review about the aptasensor for quantitative detection of kanamycin [48], more recently, Gaudin et al. reported a comprehensive review about the biosensors for the screening of antibiotic residues [26]. However, to the best of our knowledge, there were no reviews reported the TCs detection. Meanwhile, most of these papers reviewed biosensors, few of them described the chemosensors for the antibiotics detection. In addition, sensors for TCs detection are developed very fast in recent years. Numerous highly sensitive and selective sensors have appeared. It is very necessary to summarize a review for the TCs detection based on sensors. Therefore, we summarized the current research literatures on sensors for TCs detection. Those recent advances in TCs sensors are shown in Scheme 1. To highlight the recent progress in sensors for TCs detection, this review discussed the various recent development of emerging TCs sensors and its mechanisms. Furthermore, the real application of those sensors for TCs detection was focused in this review. Finally, the conclusion and challenges facing TCs sensors and future directions are concluded.

2. Optical-based tetracycline antibiotics sensors

Optical analysis methods, as excellent analysis tools, are widely used in antibiotic detection because of high sensitivity, quick response and simple use [49]. Optical sensors are usually divided into five main classes including colorimetry, fluorescence, surface Plasmon resonance (SPR), chemiluminescence (CL) and surface-enhanced Raman scattering (SERS) [48].

In this part, we summarized optical sensors for TCs detection based on different kinds of detection methods including colorimetry, SPR, fluorescence, CL and SERS. A summary of the optical-based tetracycline antibiotics sensors are provided in Table 1.

2.1. Colorimetric-based tetracycline antibiotics sensors

Among different sensing techniques, colorimetry is a comprehensive method for analytical applications due to its simplicity, low cost and practicality [50,51]. The target molecules can be detected by the naked eye is its unique advantage. The key principle of colorimetric method is transferring the detection events into color change [50]. Metallic nanoparticles such as gold and silver nanoparticles have received much attention for using in colorimetric sensors because of distance/size-dependent optical properties

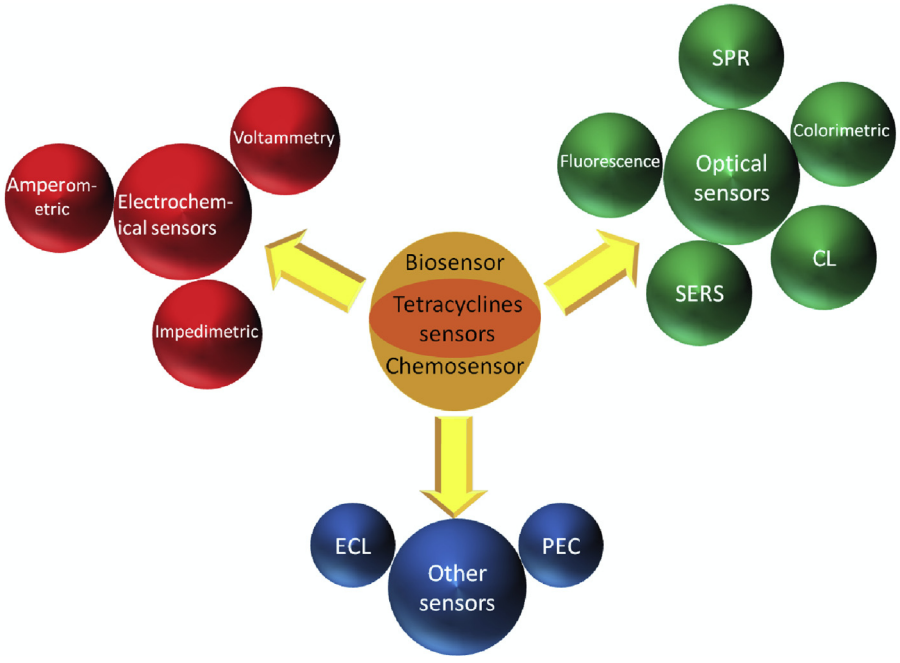

Scheme 1. General schematic of recent advances in sensors for tetracyclines detection and reviewed in this paper. SPR: surface Plasmon resonance; CL: chemiluminescence; SERS: surface-enhanced Raman scattering; ECL: electrochemiluminescence; PEC: photoelectrochemical.

Table 1
Summary of recently optical-based tetracycline antibiotics sensors.

Optical sensor types	Analytes	Signal transducer	Receptor	Linear range (μM)	LOD (μM)	References
Colorimetric	oxytetracycline	AuNPs	aptamer	0.025–1	0.025	[39]
	tetracycline	AuNPs	aptamer	–	0.0279	[57]
	oxytetracycline	AuNPs	aptamer	–	0.0001	[58]
	tetracycline	AuNPs	aptamer	0.0005–0.01	2.66×10^{-4}	[38]
	tetracycline	AuNPs	–	0.95–29.25	0.38	[61]
	oxytetracycline	AuNPs	–	0.85–32.25	0.34	
	chlortetracycline	AuNPs	–	0.88–27.15	0.35	
	doxycycline	AuNPs	–	0.87–43.67	0.52	
	oxytetracycline	TMB	enzyme	0.05–1	0.026	[43]
	tetracycline	TMB	enzyme	0.01–1	0.045	
	doxycycline	TMB	enzyme	0.05–1	0.048	
	tetracycline	AuNPs	aptamer	0.01–0.4	0.0458	[59]
	oxytetracycline	AuNPs	–	1.19–17.84	0.169	[62]
	doxycycline	AuNPs	–	0.12–1.37	0.0179	
	oxytetracycline	AuNPs	aptamer	4.01–56.43	0.458	[60]
Fluorescence	oxytetracycline	TGA@CdTe-QDs	TGA	13.4–134	0.0308	[69]
	tetracycline	CdTe-QDs	antibody	0.0225–56.25	1.13×10^{-5}	[47]
	tetracycline	MIP-MPS-QDs	MIP	–	0.45	[74]
		MIP-APS-QDs	MIP	0.12–0.37	0.54	
		MIP-MAA-QDs	MIP	0.10–0.37	0.50	
	tetracycline	QDs/MS/MIP	MIP	112.5–225	0.0113	[46]
	tetracycline	CDs-ACA	ACA	25–15000	0.05	[79]
	tetracycline	CDs/MIP	MIP	0.02–14	0.00548	[80]
	oxytetracycline	CDs	–	0.1–2.7	0.0228	[44]
	oxytetracycline	GO	aptamer	0.05–2.02	0.05	[40]
	oxytetracycline	GO	aptamer	0.01–0.2	0.01	[41]
	tetracycline	Eu^{3+}/SiNP	–	0.01–120	0.0054	[99]
	tetracycline	de-CDs	–	0.001–30	0.00052	[100]
	tetracycline	CDs	–	0.01–100	0.0033	[45]
	tetracycline	AA-Glutaraldehyde@ESM	AA	0.0225–22.5	0.0225	[101]
	tetracycline	Fe_3O_4@ZnS:Mn^{2+} QDs	–	0.01–0.7	0.0012	[102]
	tetracycline	AMP/Eu polymer	AMP	0.1–20	0.06	[103]
	tetracycline	THMS	aptamer	0–0.3	0.00209	[104]
	tetracycline	Eu^{3+}/AuNCs@$DNAc_{12}$	aptamer	0.01–5	0.004	[105]
	tetracycline	Eu^{3+}-AgNPs	Eu^{3+}	0.01–10	0.004	[106]
SPR	oxytetracycline	Metal-coated fiber	MIP	0–0.96	0.001	[85]
	tetracycline	AgNPs	–	112.5–11250	29.25	[86]
	tetracycline	GNS	aptamer and antibody	10^{-11}–0.5	10^{-11}	[87]
CL	oxytetracycline	ABEI-AuNFs	aptamer	0.0001–0.01	4.03×10^{-8}	[91]
	tetracycline	ABEI-AuNFs	aptamer	0.00011–0.0113	4.5×10^{-8}	
	tetracycline	MCLA-Ce(IV)	–	10^{-7}–2×10^{-5}	2×10^{-8}–5×10^{-8}	[92]
SERS	tetracycline	Au/PATP/SiO_2	aptamer	2.25×10^{-5}–0.225	2.25×10^{-5}	[93]
	oxytetracycline	AuNPs	aptamer	9.27×10^{-11}–9.27×10^{-7}	8.77×10^{-12}	[98]

TMB: 3,3′,5,5′-tetramethylbenzidine; TGA@CdTe-QDs: thioglycolic acid capped CdTe quantum dots; MIP-MPS-QDs: Molecularly imprinting polymer-3-Mercapto-propyltriethoxysilane-CdTe quantum dots; MIP-APS-QDs: Molecularly imprinting polymer-3-Mercapto-propyltriethoxysilane-CdTe quantum dots; MIP-MAA-QDs: molecularly imprinting polymer-methacrylic acid-CdTe quantum dots; QDs/MS/MIP: quantum dot/mesoporous silica/molecularly imprinted polymer; CDs-ACA: carbon quantum dots-triammonium citrate; CDs/MIP: carbon quantum dots/molecularly imprinted polymer; Eu^{3+}/SiNP: europium functionalized silicon nanoparticle; de-CDs: dually emitting carbon dots; AA-glutaraldehyde@ESM: anthranilic acid immobilized on eggshell membrane with glutaraldehyde; Fe_3O_4@ZnS:Mn^{2+} QDs: Fe_3O_4 nanoparticles capped Mn-doped ZnS QDs; AMP/Eu polymer: adenosine monophosphate capped europium ion; THMS: triple-helix molecular switch; Eu^{3+}/AuNCs@DNAc12: EuTC with DNA-templated gold nanoclusters; Eu^{3+}-AgNPs: Eu-citrate stabilized AgNPs; GNS: gold nanostars; ABEI-AuNFs: N-(4-aminobutyl)-N-ethylisoluminol functionalized flowerlike gold nanostructures; MCLA-Ce(IV): methoxylated cypridina luciferin analogs and Ce(IV); Au/PATP/SiO_2: AuNPs coated p-aminothiophenol with SiO_2.

[37,48,51]. Moreover, gold nanoparticles (AuNPs) show unique characteristics, such as higher extinction coefficients than organic dyes, ease of synthesis and modification which enhances the selectivity and sensitivity of colorimetric sensors [52–54].

Aptamers are single-stranded oligonucleotides, acquired by an *in vitro* process named SELEX (systematic evolution of ligands by exponential enrichment) [55]. They bind tightly to the targets ranging from small matters to proteins, antibiotics and even entire cells with high affinity and specificity. Aptamers possess ideal advantages over antibodies such as excellent thermal stability, low cost, ease of modification and production, and lack of immunogenicity and toxicity [30,34,56]. Owing to these unique properties, aptamers have attracted extensive attentions for application in biosensors.

Combination of aptamer as the bioreceptor element along with AuNPs as the signal transducer has been widely used in TCs detection [38,39,57–59]. Kim et al. [39] reported a fast and simple colorimetric assay using unmodified AuNPs and 76 per oxytetracycline-aptamer (OTC-aptamer) for detecting OTC with a linear range from 2.5×10^{-2} μM to 1 μM and a detection limit of 2.5×10^{-2} μM. In this colorimetric biosensor, the OTC-aptamer was absorbed on the surface of AuNPs by the electrostatics interaction between the bases of single-stranded DNA (ssDNA) and AuNPs, which provided the stability of nanoparticles against salt-induced aggregation because of steric effect. But with the addition of OTC, it could resulted in separation of OTC-aptamer from AuNPs surface due to OTC bound to the aptamer. Thus, upon the addition of NaCl solution, unmodified AuNPs happened to aggregation, and resulting in the color changed from red to purple even blue. Thus, a significant increased in the absorbance at 650 nm and decreased at 520 nm could be observed which realized quantitative detection of OTC. Based on the same principle, Wang and colleagues developed a 40 per tetracycline-aptamer (TC-aptamer) for highly sensitive determination of TC. In this work, they found that 76-per aptamer

was weak to protect the AuNPs from aggregation compared with 40-mer aptamer at the same concentrations. To protect the AuNPs from aggregation, higher concentration of 76-mer was needed than the 40-mer aptamer. And when aptamer is the recognition event in the detection system, high concentration of the aptamer will lead to high detection limit. In this work the detection limit of TC was lower than 2.79×10^{-2} μM [57]. More recently, Kwon et al. successfully truncated the shortened 8-mer ssDNA aptamer for four different TCs with high affinity. And the authors used the shortened 8-per aptamer (5′-CGGTGGTG-3′) for ultrasensitive colorimetric determination of OTC. The results showed that this ultrasensitive determination of OTC down to 1×10^{-4} μM was possible by using the shortened 8-mer ssDNA aptamer, which was about 500-fold enhanced compared to that acquired using the original 76-mer aptamer [58].

Except for single-stranded structure, aptamers can be able to design to other structures with advantages through base pairing. In one study, a colorimetric triple-helix molecular switch (THMS) system was designed for the first time to detect TC based on AuNPs and aptamer [38]. THMS presents unique advantages over known double-helix DNA molecular switches and molecular beacon-based signaling aptamers including high sensitivity and stability and preserving the specificity and affinity of the original aptamer. In their work, the THMS system consists of a tetracycline-aptamer (TC-aptamer) sequence with two arm segments and a dual-labeled oligonucleotide as a signal transduction probe (STP). In the absence of TC, THMS was stable. So the THMS could not protected AuNPs against salt-induced aggregation, due to its very stable structure. The color of AuNPs changed from wine red to purple or blue, after the addition of NaCl solutions. However, in the presence of TC, inducing the change of THMS structure due to the formation of TC/aptamer. THMS was broken up and released STP which adsorbed on the surface of AuNPs by electrostatic interaction between the negatively charged AuNPs and the positively charged bases of STP. Hence, AuNPs were stabilized by the STP against salt-induced aggregation and remained red (see Fig. 1). The linear range of this colorimetric biosensor was in the range of 3×10^{-4}–1×10^{-2} μM, and the limit of detection (LOD) was as low as 2.66×10^{-4} μM.

Among the advantages of aptasensor, there are other non-aptamer (N-aptamer) colorimetric chemosensors for highly sensitive detection of TCs [43,60–62]. Unlike the aptasensor, N-aptamer colorimetric chemosensors can simultaneously detect several kinds of TCs. Shen and groups [61] designed a rapid and simple colorimetric assay for the determination of four kinds of TCs using the TCs in liquid samples based on in situ growth of AuNPs. When $HAuCl_4$ mixed up with TCs, after 10 min of incubation at 70°C, a wine red color of AuNPs was observed. The absorption peak of TCs incubated AuNPs occurred at 526 nm, and the absorbance was directly associated with the concentration of TCs. The LODs of this colorimetric method were 0.38 μM, 0.34 μM, 0.35 μM, and 0.52 μM for TC, OTC, CTC, and DC, respectively.

Another novel N-aptamer colorimetric chemosensor for detection of TCs based on the catalytic activity of Fe_3O_4 magnetic nanoparticles (Fe_3O_4 MNPs) was developed by Wang et al. [43]. Different from AuNPs-based colorimetric sensors, the principle of this assay is based on Fe_3O_4 MNPs catalyze the H_2O_2-mediated oxidation of colorless 3, 3′, 5, 5′-tetramethylbenzidine (TMB) into blue product (oxTMB) as an indicator. In this chemosensor, owing to the multiple N– and O– containing groups, TC molecules had a strong ability to complex with Fe (II) or Fe (III) on the surface of Fe_3O_4 MNPs. The obtained mixture of TCs and Fe_3O_4 MNPs could resulted in the accelerated catalyzing H_2O_2-mediated oxidation of TMB by Fenton chemistry [63,64]. As a result, comparing to the similar detection system without TCs molecules, a more obvious color change of solution could be discovered. They applied this colorimetric chemosensor to detect TC, OTC, and DC with LODs of 4.5×10^{-2} μM, 2.6×10^{-2} μM, and 4.8×10^{-2} μM, respectively.

2.2. Fluorescent-based tetracycline antibiotics sensors

The fluorescent sensors are becoming increasingly popular for determination of antibiotics especially TCs, owing to their inherent characteristics, such as high efficiency and sensitivity, easy operation, and nondestructive nature [40]. Fluorescence sensors are usually constitutive of a fluorophore and a quencher to form a forester resonance energy transfer (FRET), in which identify target leading to distance-dependent fluorescence quenching or opening [34,65]. Some fluorescent probes have been used to detect TCs including quantum dots (QDs), carbon dots (CDs), europium ion (Eu^{3+}), carbon nonmaterials, and so on [66].

QDs have attracted huge amount of interest for detection of TCs due to their unique electronic and optical properties, such as photostability, narrow and symmetric spectra, low background noise, and high luminescence [32,34,67,68]. Gao et al. [69] designed a thioglycolic acid (TGA) functionalized CdTe QDs (TGA-CdTe QDs) fluorescent chemosensor for detection of OTC. In this work, the electrostatic interaction between OTC and TGA-CdTe QDs, resulting in effective electron transfer from OTC to QDs could be responsible for fluorescence quenching of CdTe QDs. Under the optimal conditions, the fluorescent chemosensor exhibited a linear range of 13.4–134 μM with a detection limit of 3.08×10^{-2} μM. Furthermore, Song et al. [47] also developed a CdTe-QDs fluorescent assay for TC detection. Compared with previous study [69], this

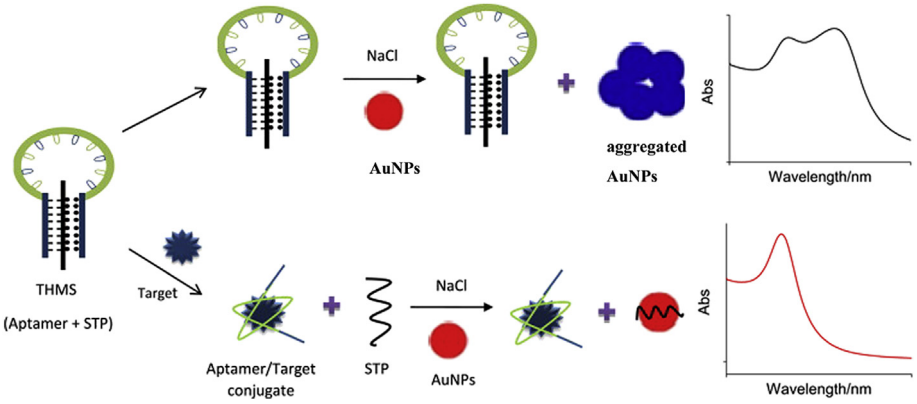

Fig. 1. Colorimetric biosensor for detection of tetracycline based on AuNPs and triple-helix molecular switch. Adapted from the published works of [38] with a little modification.

developed fluorescent chemosensor had lower linear range of 2.25×10^{-5}–5.63×10^{-2} μM and detection limit of 1.13×10^{-5} μM.

Except for conventional QDs materials, the combination of QDs with MIP can observably improve the sensitivity and selectivity [70–72]. MIP creates binding sites and receptor-specific recognition that are complementary to a template analyte [71,73]. Coating MIPs on the surface of nanoparticles improves their template-binding kinetics and increases their surface area-to-volume ratios. Three MIP-QD composites, MIP-MPS (3-mercapto-propyltriethoxysilane)-QDs, MIP-APS (3-aminopropyltriethoxysilane)-QDs, and MIP-MAA (methacrylic acid)-QDs were designed by Chao et al. [74] for fluorescence detection of TC. The detection limits were 0.45 μM, 0.54 μM, and 0.50 μM for MIP-MPS-QDs, MIP-APS-QDs, and MIP-MAA-QDs, respectively. Furthermore, Zhang et al. [46] reported a novel fluorescent chemosensor based on the hybrid quantum dot/mesoporous silica/molecularly imprinted polymer (QD/MS/MIP) for the detection of TC. In their work, mesoporous silica used as the carrier of molecularly imprinting sites, which accelerated the speed of separation and adsorption and further enhanced the imprinted molecules to combine with the mesoporous material pore wall for rapid point position recognition. In the absence of TC, the electron of QD/MS/MIP was motivated from valence band to the conduction band when accepting the ultraviolet photon. Subsequently, the motivated electron goes back to valence band, and the QD/MS/MIP generated the fluorescent signal. On the contrary, in the presence of TC, owing to the hydrogen bonding interaction between the hydroxyl groups of TC and amino groups of QDs. The strongly interaction force produced the electron transfer between QDs and TC. The energy of QDs would then transfer to the composite of QD/MS/MIP and TC, which resulted in its fluorescence quenching and with no fluorescent signal generation. Under the optimal conditions, the linear detection range was found to be 0.113–2.25 μM and a LOD of 3.375×10^{-2} μM was achieved. Furthermore, this designed chemosensor was successfully applied to detect TC in serum samples. Figs. 2–8.

Carbon quantum dots (CQDs) or carbon dots (CDs) have recently attracted considerable interest due to their excellent advantages over conventional inorganic semiconductor QDs, such as bright fluorescence, convenient synthesis, good biocompatibility and stability, excellent water solubility, easy surface functionalization, and low cytotoxicity [75–78]. Owing to these superior advantages, CQDs or CDs provided a new platform for determination of TCs. Hou and co-workers [79] reported a novel microwave-assisted method of CDs prepared from triammonium citrate (CDs-ACA) for the detection of TC. In this work, when TC was introduced, it could recombined with the ground state of the organic groups on the surface of CDs, which produced a decrease of the photoluminescent intensity. This developed chemosensor showed a LOD down to 50 nM. Based on this work, Hou et al. [80] further combined the CDs with MIP. The CDs/MIPs composites showed high extraction efficiency, good sensitivity and selectivity, and more accessible sites for the detection of TC. Furthermore, the presented assay had great potential applications for the recovering, preconcentration and direct detection of trace TC in milk samples simultaneously without secondary pollution. Under optimal conditions, the developed fluorescent chemosensor exhibited a linear range from 2×10^{-2} μM to 14 μM and with a LOD down to 5.48×10^{-3} μM.

An et al. [44] developed a water-soluble fluorescent CDs using tannic acid as carbon source for sensitive detection of OTC. The as-prepared CDs were functionalized by catechol molecules in the synthesis of particle. Owing to the coordination binding between Fe^{3+} and catechol groups on the surface of CDs, which lead to the fluorescence emission of CDs gradually decreased with increasing Fe^{3+} ions. However, in the presence of OTC, the fluorescence of pre-quenched CDs were then gradually recovered owing to the competition coordination between Fe^{3+} and OTC. This developed fluorescent chemosensor could be used for detecting OTC in a linear range of 0.1–2.7 μM with a LOD of 2.28×10^{-2} μM, and was applied to detect OTC in real milk samples.

Among the large family of fluorescent-based quenchers, graphene oxide (GO) is the most usually used fluorescent materiel in view of its excellent fluorescence quenching ability, water solubility, and easy synthesis [40,41]. For example, Tan and co-workers [40] developed a GO hydrogel-based fluorescent assay for OTC detection. The GO hydrogel was prepared by physically mixing aptamers, GO sheets and adenosine together, in which the aptamer and adenosine work as the co-cross-linkers to connect the GO sheets and then form the three-dimensional macrostructures. Under the optimal conditions, the designed fluorescent biosensor had a linear range of 5.04×10^{-2}–2.02 μM with a LOD down to 5.04×10^{-2} μM. Moreover, they applied this fluorescent method to detect OTC in real water samples with good accuracy.

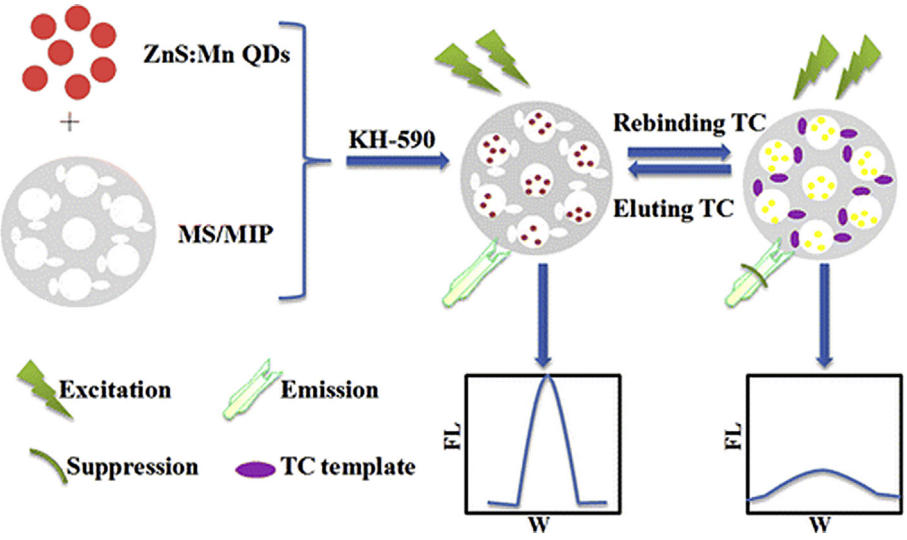

Fig. 2. Fluorescence chemosensor based on hybrid mesoporous silica/quantum dot/molecularly imprinted polymer for detection of tetracycline. Reprinted with permission from Ref. [46].

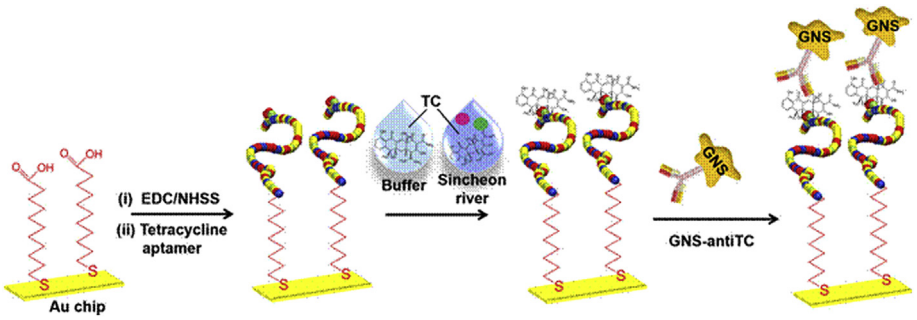

Fig. 3. Schematic illustration of SPR biosensor for tetracycline detection. The tetracycline aptamer was first immobilized on an Au chip, followed by the covalent attachment of aptamer probes. Tetracycline binding was performed in both buffer and Sincheon river samples, followed by the subsequent binding of GNS-antiTC's for further SPR signal amplification. Reprinted with permission from Ref. [87].

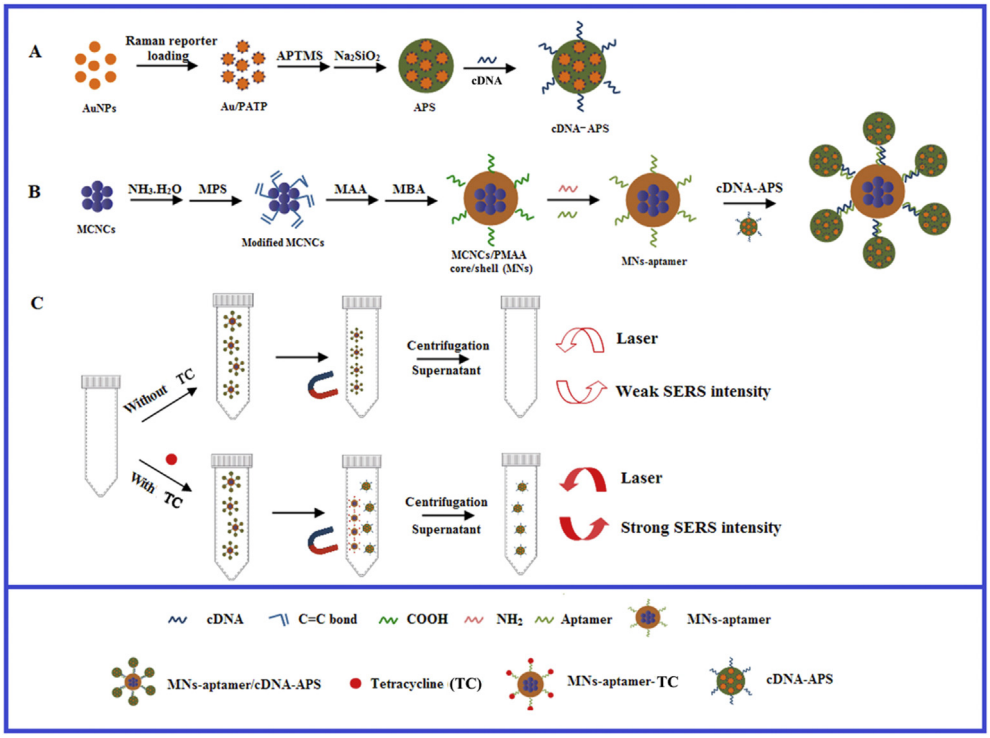

Fig. 4. Schematic illustration of fabrication process of MNs-aptamer/cDNA-APS probe (A, B); Schematic illustration of the detection process of MNs-aptamer/cDNA-APS probe based SERS biosensor (C). Adapted from the published works of [93] with a little modification.

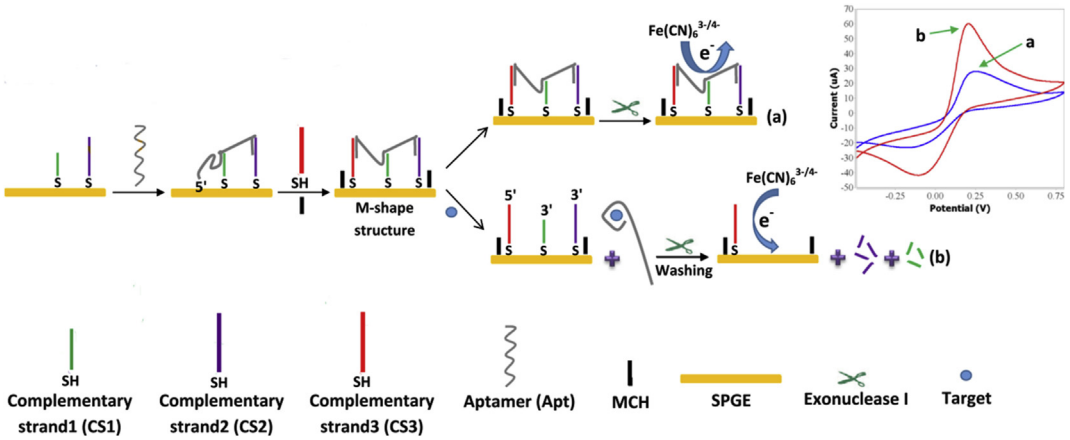

Fig. 5. Schematic illustration of tetracycline detection based on electrochemical method. In the absence of tetracycline, the M-shape structure of CSs-Apt complex remains intact and redox probe could not have access to the surface of electrode, leading to a weak electrochemical signal (a). In the presence of tetracycline, Apt binds to tetracycline and leaves the CSs. Exo I degrades CS1 and CS2, resulting in the free access of redox mediator to the surface of electrode and a strong electrochemical signal (b). Adapted from the published works of [109].

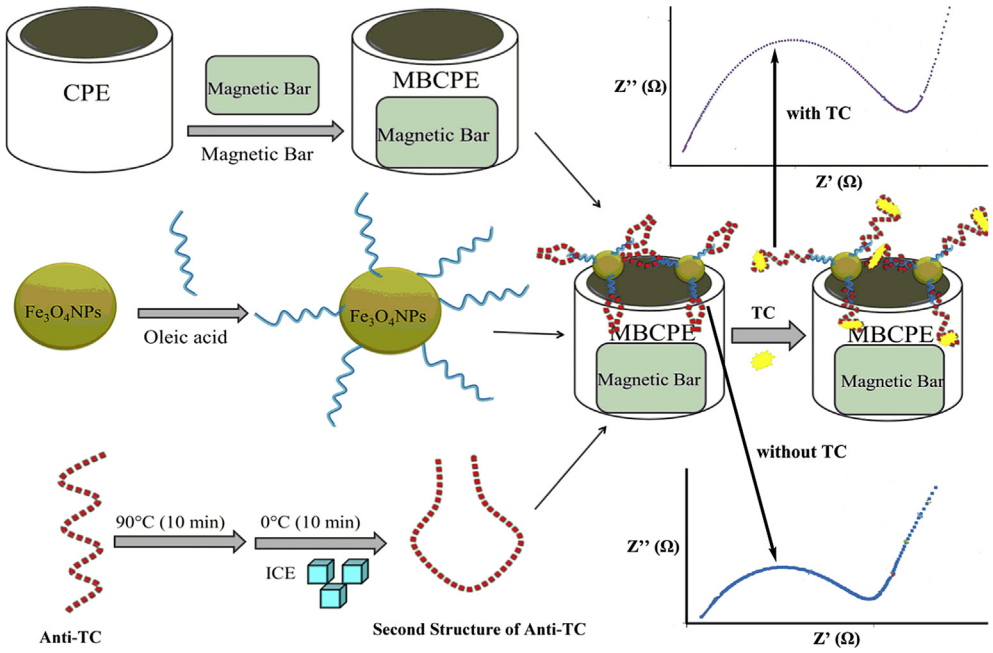

Fig. 6. Schematic illustration of MBCPE/Fe_3O_4NPs@OA/*anti*-TET electrochemical aptasensor for the detection of tetracycline. Adapted from the published works of [115] with a little modification.

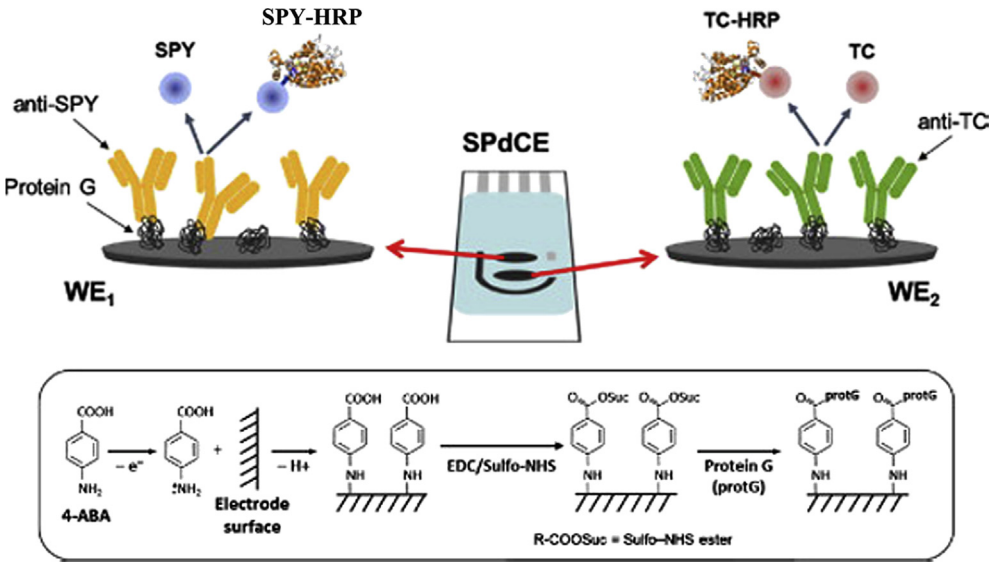

Fig. 7. Schematic illustration of Protein G-modified screen-printed dual carbon electrodes (SPdCEs) electrochemical immunosensor for the detection of tetracyclines and sulfonamides. Adapted from the published works of [122].

2.3. Surface Plasmon resonance-based tetracycline antibiotics sensors

In the past decades, surface Plasmon resonance (SPR) sensors have attracted extensive attention in antibiotics detection due to their compact design, low-cost, and more importantly their ability to realize the label-free and real-time analysis [81,82]. The SPR sensor with outstanding excellent reproducibility and reutilization performance has become increasingly popular in environmental monitoring, food safety, and drug discovery, especially for point-of-care diagnostics [83]. SPR is the phenomenon of oscillation that exists at the interface between two materials, which could be induced by both electrons and photons. It is very sensitive to the refractive index of the dielectric that is attached to the metal surface. Since the refractive index was the inherent feature of all materials, any dielectric attached to the metal surface has been able to be detected [84]. Generally, SPR sensors employ MIP or antibodies as receptors to capture its corresponding target because of their superior performance [84].

For example, Verma et al. [85] developed a optical TCs chemosensor using SPR technique along with molecule imprinting. In their work, the MIP was used for the preparation of the recognition element, while the SPR technique was used as the transducer. The MIP produced specific binding sites with functional groups that are

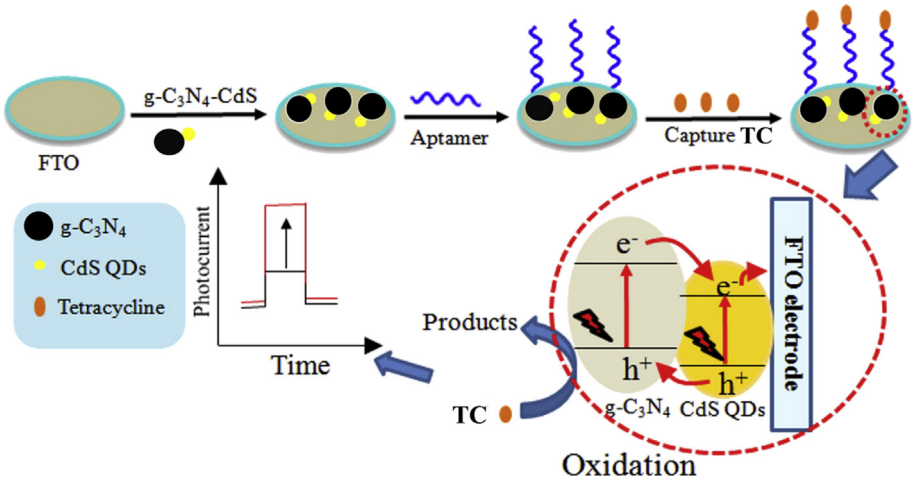

Fig. 8. Schematic illustration of graphitic carbon nitride (g-C_3N_4) coated with CdS QDs for visible-light-driven photoelectrochemical detection of tetracycline. Adapted from the published works of [138].

recognition the target molecules such as TC and OTC. When the TC or OTC binds on the recognition element, the interfacial architecture changed and the surface Plasmon became exciting, generating a readable optical signal. This designed chemosensor exhibited a linear range of 0–0.96 μM. Moreover, a simple and sensitive SPR assay for the detection of TC based on its reducing $AgNO_3$ to silver nanoparticals (AgNPs) in alkaline medium containing sodium hydroxide and ammonia at 65°C was designed by Amjadi et al. [86]. The Plasmon absorption peak of the formed AgNPs occurred at 411 nm was proportional to the TC concentration. Under the optimized conditions, the linear range was found to be 0.225–4.5 μM and the LOD was 2.93×10^{-2} μM.

Kim and co-workers [87] have very recently developed a gold nanostar (GNS) enhanced SPR bio-affinity biosensor using a new DNA aptamer-antibody sandwich method for determination of TC. The TC aptamer was first absorbed on the Au SPR chip via covalent coupling with 11-mercaptoundecanoic acid (MUA). Then, TC was absorbed on the surface of TC aptamer-modified Au chip and performed in buffer solutions and Sincheon river samples, respectively. The SPR signal was further amplified by the specific binding of tetracycline antibody (antiTC) through formation of a sandwich assay format. Under the optimized conditions, this SPR biosensor with the linear range from 0.5 μM down to 1×10^{-11} μM and the LOD was as low as 1×10^{-11} μM. Furthermore, the developed SPR biosensor was successful applied to the river samples for the determination of TC.

2.4. Chemiluminescent-based tetracycline antibiotics sensors

Owing to its attractive advantages of operational simplicity, low cost of detection, high sensitivity as well as sampling rate, chemiluminescence (CL) method plays an important and powerful role in analytical technique [88]. CL-based detection method is widely applied to different fields, especially in optical biosensor assays [89]. CL is substance absorption of chemical energy produce light radiation in the process of chemical reactions [88]. Compared with the fluorescence method, CL has several advantages such as no requirement for an external light source, a simple sensor setup, and longer life time than that of fluorescent ones [90].

CL-based sensor has recently been applied to the detection of TCs. For example, Hao and co-workers [91] designed a novel multiplex chemiluminescent aptasensor for simultaneous detection of three antibiotics including TC, OTC, and kanamycin (KA). In this study, they used the thiolated hybridized complementary strand (cDNA) modified N-(4-aminobutyl)-N-ethylisoluminol (ABEI) functionalized flower-like gold nanostructures (AuNFs) as signal probes. In the absence of targets, the flower-like AuNFs had a maximum CL intensity. However, in the presence of targets, owing to the weaker interaction of aptamer/DNA duplex than that of aptamer/targets the aptamer tended to bind with target and induced the signal probes washed away. As a result, the CL intensity was correlated with the concentration of targets. On the basis of this competitive mechanism, the linear ranges were 1.12×10^{-4}–1.13×10^{-2} μM, 1×10^{-4}–1×10^{-2} μM, and 1.01×10^{-4}–1.01×10^{-2} μM, and the LOD were 4.5×10^{-5} μM, 4.2×10^{-5} μM, and 3.4×10^{-5} μM, respectively. Moreover, this developed highly sensitive CL assay could be successfully used for the determination of three antibiotics in milk. Another ultrasensitive CL biosensor for the detection of TCs was designed by Zeng at al [92]. The developed CL method had a linear range from 1×10^{-7} μM to 2×10^{-5} μM and LOD of 2×10^{-8}–5×10^{-8} μM.

2.5. Surface-enhanced Raman scattering-based tetracycline antibiotics sensors

Surface-enhanced Raman scattering (SERS) sensors have promising potential in the field of tetracycline antibiotics detection because of their non-invasive probing, ultrahigh detection sensitivity, minimal sample preparation, compatibility with aqueous solution, and label-free monitoring for specific analyte in complex matrices [93,94]. SERS sensors based on the magnitude of Raman scattering signal can be greatly enhanced when scatterer was placed on or near a roughened noble-metal substrate [95]. Recently, SERS-based sensor has been used in practical application of TCs detection [96,97].

Li et al. [93] designed a sensitive and rapid SERS-based magnetic nanospheres-targeting biosensor for detection of TC using aptamer-conjugated magnetite colloid nanocrystal clusters (MCNCs)-polymethacrylic acid (PMAA) magnetic nanospheres (MNs) as the recognition and Au/PATP/SiO_2 (APS) as the labels. Firstly, aptamers were fabricated and conjugated into the MNs' surfaces through condensation reaction. The MNs possessed of excellent biocompatibility and high saturation magnetization (Ms), which rapidly and easily facilitated the magnetic separation. Then, APS nanocarrier loaded with complementary DNA (cDNA) to generate a large amplification factor of Raman signals. Owing to the

hybrid reaction between aptamers and cDNA, APS nanocarrier was immobilized on the surface of MNs and thus the MNs-targeting aptasensor was fabricated. Next, TC bound successfully to the aptamer upon it addition with the subsequent release of some cDNA-APS into the bulk solution. Under magnet attraction, the nanospheres were deposited together. Consequently, a display of strong SERS signals by supernatants of the resulting mixtures with increasing TC concentrations was observed. The proposed aptasensor showed excellent performances for TC detection along with wide linear range of 2.25×10^{-6}–2.25×10^{-1} μM, low detection limit of 2.25×10^{-6} μM, high sensitivity, and good selectivity to the general coexisted interferences.

Another ultrasensitive SERS biosensor for determination of OTC was proposed by Meng et al. [98]. The designed method was constructed on the basis of Raman hot spot between AuNPs (13 nm and 80 nm diameter respectively) linked by a DNA sequence. The DNA sequence combined with the OTC aptamer including its complementary sequence as well as a stem-loop structure. The Raman signal molecule (4-MBA) was modified on the surface of 13 nm AuNPs. After the exposure of OTC, the aptamer sequence was preferentially combined with OTC and partially dehybridized with its complementary sequence which lead the 13 nm AuNPs to get closer to the 80 nm AuNPs. The Raman intensity was thus increased for the more enhanced hot spot generated. Under the optimal experimental conditions, the SERS signal was positively related to the OTC concentration with a wide working range of 9.27×10^{-11}–9.27×10^{-7} μM and the LOD was as low as 8.77×10^{-12} μM. The recovery rates of fishmeal ranged from 91.29 to 110.98%. The specificity of this method was further examined, and the results showed that the AuNPs based aptasensor was highly selective.

3. Electrochemical-based tetracycline antibiotics sensors

Electrochemical sensors have been widely used in the area of analysis (including metal ions, antibiotics, stimulants etc) [107,108]. Owing to their unique properties, such as rapid reaction, simplicity, and low cost compared with conventional methods, electrochemical sensors are drawing more attention in the detection of antibiotics. Moreover, compared to optical sensors (colorimetric and SPR sensors), electrochemical sensors have lower detection limit. The basic principle of electrochemical sensors is that chemical reactions between target analytes and immobilized identification molecules generate or consume electrons or ions, which affects the measurable electrical properties of the work electrode, such as potential or electric current or resistance [25,32,67]. According to different types of measurable electrical properties, electrochemical sensors can be classified into voltammetric, impedimetric and amperometric sensors. A summary of the reports on electrochemical-based tetracycline antibiotics sensors are provided in Table 2.

3.1. Voltammetric sensors

Voltammetric strategy shows excellent sensitivity and selectivity due to the analyte can be easily recognized by its voltammetric peak potential [109]. There are two main types of voltammetric techniques including differential pulse voltammetry (DPV) and cyclic voltammetry (CV) [110]. These techniques are all widely applied to electrochemical sensors for determination of TCs (see Table 2).

Taghdisi et al. [109] designed a novel electrochemical biosensor using DPV technique for selective and ultrasensitive detection of TC which was based on gold electrode, M-shape structure of aptamer (Apt)-complementary strands of aptamer (CSs-Apt) complex, and exonuclease I (Exo I). In the absence of TC, the M-shape structure which acted as a barrier and gate for the access of redox probe to surface of gold electrode remains intact, resulting in a weak electrochemical signal. Upon addition of TC, aptamer combined with TC and left CSs-Apt, leading to disassembly of M-shape structure and a strong electrochemical signal was appeared with followed the addition of Exo I. Exo I degrades CS1 and CS2, resulting in the free access of electrochemical probe of $Fe(CN)_6^{3-/4-}$ to the surface of electrode and a strong electrochemical signal. The designed analytical method revealed high selectivity toward TC with a LOD was as low as 4.5×10^{-2} μM. Moreover, the developed biosensor was effectively used for the determination of TC in serum and milk samples with LODs of 7.1×10^{-2} μM and 7.4×10^{-2} μM, respectively.

An electrochemical biosensor based on multi-walled carbon nanotubes (MWCNTs) modified GCE using DPV and CV techniques for the determination of TC was reported by Zhou et al. [111]. The *anti*-TC aptamer fixed on the surface of carboxyl functionalized MWCNTs and then the aptasensor was constructed. The specific identification of TC and aptamer was investigated by the electrochemical probe of $Fe(CN)_6^{3-/4-}$. After pretreated, the GCE was modified with MWCNTs, the peak current of MWCNTs modified GCE changed obviously, which was as triple as the bare GCE, indicating that the introduction of MWCNTs played an important role in the increase of the electroactive surface area and conductibility of the biosensor. Under the optimal conditions, the linear range was found to be 0.01 μM–50 μM with a LOD down to 5×10^{-3} μM. Furthermore, the biosensor was successfully applied to detect tetracycline in spiked milk samples.

3.2. Impedimetric sensors

Electrochemical impedance spectroscopy (EIS) is a label-free technique, and it is not needed to modify the interest biomolecules with markers such as fluorescent dyes, enzymes, or other redox labels [112]. Also, this technique possesses other benefits such as ease of signal quantification, excellent sensitivity, and ability to separate the surface binding events from the solution resistance [113]. But this technique is so sensitive to the electrode surface changes so the selectivity is lower than some electrochemical techniques such as DPV. Compared with other techniques, EIS possesses advantages such as easy of signal amplification and high sensitivity [114]. In the past few years, EIS technique has been widely used in sensing for TCs detection because of their fast detection and excellent sensitivity [115–120].

Jajanbani et al. [115] proposed two aptasensors based on the modified carbon paste electrode (CPE). Oleic acid (OA) modified CPE (CPE/OA/*anti*-TC), and Fe_3O_4 magnetic nanoparticles and oleic acid modified magnetic bar carbon paste electrode (MBCPE/Fe_3O_4 MNPs/OA/*anti*-TC). In this study, the developed two aptasensors both using EIS and DPV techniques for the detection of TC (see Table 2). Interestingly, the CPE/OA/*anti*-TC aptasensor with a linear range of 1.0×10^{-6}–1.0×10^{-1} μM and a LOD of 3.0×10^{-7} μM by EIS technique, and a linear range of 1.0×10^{-4}–1.0×10^{-1} μM and a LOD of 2.9×10^{-5} μM by DPV technique, respectively. Furthermore, the linear range and LOD of MBCPE/Fe_3O_4 MNPs/OA/*anti*-TC aptasensor were found to be 1.0×10^{-8}–1.0 μM and 3.8×10^{-9} μM respectively by EIS technique, and 1.0×10^{-6}–1.0 μM and 3.1×10^{-7} μM respectively by DPV technique. The results showed that EIS technique has more widely linear range and lower LOD compared with DPV technique. Meanwhile, it is noticeable that using the synthesized nanomaterials of Fe_3O_4 MNPs and Fe_3O_4 MNPs@OA resulted in performing a better immobilization process at the electrode surface. The electrochemical signal of this aptasensor originated from the soluble redox probe of $Fe(CN)_6^{3-/4-}$.

Table 2
Summary of recently electrochemical-based tetracycline antibiotics sensors.

Electrochemical sensor types	Electrode	Analytes	Technique	Receptor	Linear range (μM)	LOD (μM)	References
Voltammetric	M-shape of aptamer/SPGEs	tetracycline	DPV	aptamer	1.5×10^{-3}–3.5	4.5×10^{-4}	[109]
	HPR/MWCNTs/CPE	oxytetracycline	DPV	enzyme	15–1500	3.5×10^{-2}	[123]
	rGO-Fe_3O_4/SPCE	tetracycline	DPV	aptamer	1–5000	6×10^{-4}	[124]
	CS–PB-CR/MWCNTs-CS/GCE	tetracycline	DPV	aptamer	0.0001–1000	5.6×10^{-6}	[125]
	MIP/MWCNTs-AuNPs/GCE	tetracycline	CV	MIP	0.225–90	0.09	[126]
	AuNPs/PB-CS-GA/GCE	tetracycline	DPV	aptamer	0.01–10, 10–10000	3.2×10^{-4}	[127]
	UV-DNA/GCE	tetracycline	CV	aptamer	0.3–90	0.27	[128]
	aptamer/GE	tetracycline	CV	aptamer	0.01–10	0.01	[129]
	MWCNTs/GCE	tetracycline	DPV	aptamer	0.01–10	5×10^{-3}	[111]
Impedimetric	OA/CPE	tetracycline	EIS	aptamer	10^{-6}–0.1	3×10^{-7}	[115]
		tetracycline	DPV	aptamer	10^{-4}–0.1	2.9×10^{-5}	
	OA/Fe_3O_4/MBCPE	tetracycline	EIS	aptamer	10^{-8}–10	3.8×10^{-9}	
		tetracycline	DPV	aptamer	10^{-6}–10	3.1×10^{-7}	
	Ab-MNPs-CS/GE	tetracycline	EIS	antibody	1.8×10^{-4}–2.25×10^{-3}	7.2×10^{-5}	[116]
	GO/GCE	tetracycline	EIS	aptamer	10^{-7}–10	2.9×10^{-8}	[117]
	aptamer/GE	tetracycline	EIS	aptamer	2.25×10^{-2}–6.75	2.5×10^{-3}	[118]
	aptamer/GE	tetracycline	EIS	aptamer	1.25×10^{-3}–11.25	2.5×10^{-4}	[119]
	nano ATO-CS/IDAMs	tetracycline	EIS	aptamer	2.25×10^{-2}–2250	6.75×10^{-3}	[120]
Amperometric	MB/*anti*-TC aptamer/DpAu/GCE	tetracycline	–	aptamer	10^{-4}–10^{3}	4.2×10^{-5}	[121]
	ProtG-EDC/NHS-4-ABA/SPdCEs	tetracycline	–	enzyme	6.4×10^{-3}–0.385	1.93×10^{-3}	[122]
		sulfapyridine	–	enzyme	1.92×10^{-3}–0.454	3.9×10^{-4}	

M-shape of aptamer/**SPGEs:** M-shape of aptamer modified screen-printed gold electrodes; **HPR/MWCNTs/GCE**: horse radish peroxidase caped multi-walled carbon nanotubes modified carbon paste electrode; **rGO-Fe_3O_4/SPCE**: reduced graphene oxide and magnetite Fe_3O_4 nanoparticles modified screen-printed carbon electrodes; **CS–PB-CR/MWCNTs-CS/GCE**: multi-walled carbon nanotubes-chitosan and chitosan-prussian blue-graphene nanoparticals modified glass carbon electrode; **MIP/MWCNTs-AuNPs/GCE**: Molecularly imprinting polymer and gold nanoparticals modified multi-walled carbon nanotubes modified glass carbon electrode; **AuNPs/PB-CS-GA/GCE**: prussian blue-chitosan-glutaraldehyde doped gold nanoparticals modified glass carbon electrode; **UV-DNA/GCE**: UV irradiated DNA film modified glassy carbon electrode; **aptamer/GE**: aptamer modified gold electrode; **MWCNTs/GCE**: multi-walled carbon nanotubes modified glassy carbon electrode; **OA/CPE**: oleic acid modified carbon paste electrode; **OA/Fe_3O_4/MBCPE**: magnetite Fe_3O_4 nanoparticles and oleic acid modified carbon paste electrode; **Ab-MNPs-CS/GE**: monoclonal antibody and Fe_3O_4 nanoparticles doped chitosan modified gold electrode; **GO/GCE**: graphene oxide modified glassy carbon electrode; nano **ATO-CS/IDAMs**: antimony tin oxide nanoparticle-chitosan modified interdigitated array microelectrodes; **MB/*anti*-TC aptamer/DpAu/GCE**: Methylene blue coated *anti*-TC aptamer modified glassy carbon electrode with electrodeposition gold nanoparticals; **ProtG-EDC/NHS-4-ABA/SPdCEs**: Protein G covalently immobilized 4-aminobenzoic modified screen-printed dual carbon electrodes.

Fe_3O_4 MNPs could accelerated the electron transfer kinetics and improved the sensitivity of EIS technique was also demonstrated by Liu et al. [116]. In addition, the developed biosensors were successfully used for the determination of TC in some real samples such as milk, drug, blood serum and honey samples.

Later, Benvidi et al. [117] reported an electrochemical aptasensor for the determination of TC based on graphene oxide nanosheets (GO) modified glassy carbon electrode (GCE). GO was used to facilitate the *anti*-TC immobilization through π-π interaction between GO and aptamer, thus improving the property of electrochemical aptasensor. In this work, the designed aptasensor also both used EIS and DPV techniques to detect TC. Under optimum conditions, the fabricated aptasensor showed a linear range of 1.0×10^{-7}–10 μM and a LOD of 2.9×10^{-8} μM by EIS technique, and linear range of 1.0×10^{-4}–100 μM and a LOD of 3.1×10^{-5} μM by DPV technique. Results also revealed that EIS technique had a more widely linear range and lower LOD compared with DPV technique. The electrochemical signal of this aptasensor originated from the soluble redox probe of $Fe(CN)_6^{3-/4-}$. In addition, the proposed aptasensor was successfully used for the determination of tetracycline in serum sample.

3.3. Amperometric sensors

Apart from the commonly voltammetric and impedimetric sensors, amperometric sensor was also an efficient electrochemical technique for detection of TCs. For example, Guo et al. [121] developed a label-free electrochemical aptasensor modified with methylene blue (MB) and electrodeposited gold nanoparticles (Ed-AuNPs) for the detection of TC by amperometric technique. The AuNPs were used to immobilize *anti*-TC aptamer and facilitate electron transfer, and MB could supplied much more adsorption sites for TC. Based on the results, the proposed electrochemical aptasensor exhibited a linear range of 1.0×10^{-4}–1.0×10^{3} μM, with a detection limit of 4.2×10^{-6} μM. Furthermore, the amperometric aptasensor was successfully employed to detect TC in milk samples.

A novel integrated electrochemical immunosensor for multiplexed detection of TCs and sulfonamide antibiotics (SAs) by using amperometric technique was reported by Conzuelo et al. [122]. It is based on the selective capture antibiotics immobilize on the surface of Protein G-modified screen-printed dual carbon electrodes (SPdCEs). In this work, the 4-aminobenzoic acid (4-ABA) film covalent immobilization of Protein G grafted on the disposable electrode, and horseradish peroxidase (HRP)-labeled tracers was used as a direct competitive immunoassay. Quantification was achieved through the electrochemical monitoring of the enzyme product at the SPdCEs, using H_2O_2 as the enzyme substrate and hydroquinone as electron transfer mediator. The proposed electrochemical immunosensor showed a very low LOD (in the low ppb level) for TCs and SAs detection. Furthermore, this electrochemical immunosensor was employed to detect TCs and SAs in milk samples with satisfactory results.

4. Other tetracycline antibiotics sensors

4.1. Electrochemiluminescence-based tetracycline antibiotics sensors

Electrochemiluminescence (ECL) is a well-known high sensitivity detection assay depending on the generation of an optical signal triggered by an electrochemical reaction [130]. ECL sensor combines the sensitivity of CL with the advantages of electrochemistry. So we put ECL sensor out of the optical and electrochemical sensor. The principle of ECL sensor was reviewed by Liu et al. [130]. Recently, ECL sensor has been widely applied to detect

TCs [131–133] (see Table 3). $Ru(bpy)_3^{2+}$-based ECL has become an extensively analysis technique due to its good electrochemical stability, high ECL efficiency, and wide linear range. There are several reports using $Ru(bpy)_3^{2+}$-based ECL sensors in determination of TCs. For example, Guo et al. [131] designed a ultrasensitive $Ru(bpy)_3^{2+}$/2-(dibutylamino) ethanol (DBAE) ECL system for the detection of four TCs. In the presence of targets, the four TCs could strongly restrained the ECL signal of $Ru(bpy)_3^{2+}$/DBAE system. Under the optimized conditions, the developed ECL chemosensor had good linear range from 9.0×10^{-5} μM to 9.0×10^{-3} μM and a LOD of 4.5×10^{-6} μM. In addition, the assay was successful used for the detection of four TCs in honey samples.

More recently, a novel ECL chemosensor based on a $Ru(bpy)_3^{2+}$-doped silica nanoparticles (Ru-SiNPs)/Nafion film modified electrode for the determination of TCs was designed by Chen et al. [132]. After being prepared by a water-in-oil microemulsion method, the Ru-SiNPs were then immobilized on the GCE with the help of Nafion film. Interestingly, compared with $Ru(bpy)_3^{2+}$/DBAE system, they found that the presence of TCs could greatly enhance the ECL signal response of the modified electrode. The results showed that the linear range was 0.1–100 μM for OTC, 1–100 μM for TC, and 1–100 μM for CTC. The LODs were 0.10 μM for OTC, 0.23 μM for TC, and 0.16 μM for CTC, respectively. Moreover, this proposed ECL sensor also revealed excellent stability and repeatability, which resulted in its application in detection of antibiotics content in drugs.

4.2. Photoelectrochemical-based tetracycline antibiotics sensors

Photoelectrochemical (PEC) sensing is a novel approach with high sensitivity and rapid response [134]. It reveals greater performance than traditional electrochemical and optical sensors because it combines the advantages of them. Owing to their significant advantages such as easy miniaturization, simple apparatus, fast response, ultrahigh sensitivity, and reduced background signal, detection methods based on PEC sensors have been paid a growing attention [135]. The working principle of PEC sensor is on the basis of the combination of the PEC oxidation and specific bio-recognition, and then produce photocurrent signal [134,135]. Recently, PEC sensor has been widely applied to detect TCs [136–139] (see Table 3).

Yan et al. designed a "signal-off" PEC aptasensor based on BiOI graphene (BiOI-G) nanocomposite for the detection of OTC [136]. In this study, the *anti*-OTC aptamer employed as the bio-recognition element and BiOI was used to produce a cathodic photocurrent signal. The photocurrent response of BiOI could be amplified by the doped a suitable amount of graphene. In the presence of OTC, the photocurrent was decreased because of the specific capture of OTC by aptamer. This developed PEC biosensor revealed a linear range from 4.0×10^{-3} μM to 0.15 μM and the LOD was found to be 9×10^{-4} μM.

Liu and coworker [138] proposed a novel graphitic carbon nitride (g-C_3N_4) sensitized with CdS QDs PEC aptasensor for determination of TC. In this work, g-C_3N_4 coupled with CdS QDs (g-C_3N_4-CdS) nanocomposites introduced as highly efficient photoactive materials while the free TC-binding aptamer was used as the special bio-recognition element. TC aptamer was able to be immobilized on the surface of g-C_3N_4-CdS composites via π-π stacking interaction. Interestingly, they found that the g-C_3N_4-CdS composites showed highly sensitive photocurrent signal responding compared with either CdS QDs or pristine g-C_3N_4 [140]. In the presence of TC, an enhanced photocurrent signal was produced due to the specific capture of TC by TC-binding aptamer. Under the optimal conditions, this developed PEC aptasensor revealed a linear range from 1×10^{-2} μM to 0.25 μM and with a detection limit of 5.3×10^{-3} μM.

Recently, Li et al. [139] developed a novel reusable PEC aptasensor for the detection of OTC based on a signal "switch off-on" strategy. In their study, the hairpin DNA probe and CdTe quantum dots (H-DNA/QDs) was immobilized on ITO/TiO_2 electrode at first. Then introduce the OTC aptamer, the hairpin DNA probe hybridized with OTC aptamer leads to CdTe QDs far away from ITO/TiO_2 electrode surface and decrease of photocurrent signal. While in the presence of OTC, the photocurrent signal of ITO/TiO_2/H-DNA/QD/aptamer recovered significantly. Under the optimal conditions, this proposed PEC aptasensor had a linear range towards OTC from 2×10^{-3} μM to 0.3 μM and with a LOD down to 1.9×10^{-4} μM. Moreover, the developed PEC aptasensor could be regenerated by adding dehydroascorbate and applied to detect OTC in complex environment water samples (tap water and lake water) or food samples (raw milk and chicken).

5. Application of sensors

The application of sensors for TCs for real samples detection is an important strategy to assess its application potential and analytical reliability. In this part we will pay more attention to samples preparation and analysis.

5.1. Samples preparation

Real samples containing food samples (milk, honey and chicken), water samples (tap water and lake water), biological samples (serum and urine) and tablets are used to evaluate the TCs

Table 3
Other tetracycline antibiotics sensors.

Sensor types	Signal transducer	Analyst	Receptor	Linear range (μM)	LOD (μM)	References
ECL	RuSiNPs/Nafion/GCE	tetracycline	RuSiNPs	1–100	0.23	[132]
		oxytetracycline		0.1–100	0.10	
		chlortetracycline		1–100	0.16	
	$Ru(bpy)_3^{2+}$/DBAE	tetracycline	DBAE	4×10^{-5}–4×10^{-3}	2×10^{-6}	[131]
		oxytetracycline		4×10^{-5}–4×10^{-3}	2×10^{-6}	
		chlortetracycline		4×10^{-5}–4×10^{-3}	2×10^{-6}	
		doxycycline		4×10^{-5}–4×10^{-3}	2×10^{-6}	
PEC	nano Au/TiO_2/ITO	tetracycline	aptamer	0.0003–1.6	1×10^{-4}	[137]
	ITO/TiO_2/AuNPs/H-DNA@QDs	oxytetracycline	aptamer	0.002–0.3	1.9×10^{-4}	[139]
	g-C_3N_4-CdS/FTO	tetracycline	aptamer	0.01–0.25	0.0053	[138]
	BiOI-G/FTO	oxytetracycline	aptamer	0.004–0.15	9×10^{-4}	[136]

RuSiNPs/Nafion/GCE: RuSiNPs/Nafion film modified glassy carbon electrode; $Ru(bpy)_3^{2+}$/DBAE: 2-(dibutylamino)ethanol co-reactant with $Ru(bpy)_3^{2+}$; nano Au/TiO_2/ITO: nano Au/TiO_2 modified Indium Tin Oxide electrode; ITO/TiO_2/AuNPs/H-DNA@QDs: hairpin DNA conjugate with CdTe QDs immobilized on the TiO_2/AuNPs modified Indium Tin Oxide electrode; g-C_3N_4-CdS/FTO: graphitic carbon nitride coupled with CdS quantum dots modified F-doped SnO_2 conducting glass; BiOI-G/FTO: p-type semiconductor BiOI doped with graphene modified F-doped SnO_2 conducting glass.

sensors. The pretreatment was described in detail are presented in below.

For milk or chicken samples [139], 1.0 mL of raw milk or 1.0 g of chopped chicken was placed into a 15 mL centrifuge tube and diluted with water to 10 mL, then 2 mL of chloroform and 2 mL of 10% trichloroacetic acid were added and mixed under vortex for 10 min to deposit protein and dissolve at and other organic substances in the sample matrix. After centrifuged at 13,000 rpm for 10 min, the supernatant was centrifuged at 10,000 rpm for 10 min to remove the sediment once again, and the supernatant was collected.

The pretreatment of the honey solution [141] was done as follows: 1.0 g of honey was added to ethanol (1 mL) and sonicated in an ultrasonic bath for 30 min. To reduce the matrix effect, the sample solution was then diluted 1/10 (v/v) with a phosphate buffer solution and filtered through a filter paper. Finally, to deposit protein and dissolve at and other organic substances the process is same with the milk, and the supernatant was collected.

For water samples [139], tap water and lake water samples were filtered through a 0.2 μm nitrocellulose membrane filter immediately after sampling. For urine samples [61], 0.1 M acetic acid was added to urine samples at a 1:2 (v/v) ratio. The mixtures were centrifuged at 5000 rpm (4°C) for 30 min, and the supernatants were collected.

For serum samples [115], proteins of serum were removed using acetonitrile. 125 mL of cold acetonitrile was added to 50 mL of serum, with gentle mixing. The mixtures were incubated for 60 min at 4°C. The samples were centrifuged at 9500 rpm for 10 min at 4°C, and the supernatant was collected.

For the OTC tablets [43], before grinding, three pieces of OTC tablets were weighted, and then the average amount of one tablet was calculated. After grinding to fine powder, the amount equal to 4.098 mg was weighted accurately, and then transferred into a 7 mL centrifuge tube. After that, ultrapure water (5 mL) was added into the tube to dissolve the powder. The solution was diluted 100 times with ultrapure water when in use.

A certain amount of TCs was added into the raw real samples, then pretreated in accordance with the above procedure.

5.2. Samples analysis

Results with real samples detection are very important. To investigate the application of the designed sensors in real samples, different concentrations of TCs are add into the raw real samples before pretreatment. Moreover, the sample dilution factor during pretreatment needs to be considered. The accuracy of the results is evaluated by the recoveries. The spiked TCs are also determined by standard ELISA or HPLC method for comparison and to validate the reliability of the proposed analytical method.

In Jajanbani's work [115], the developed aptasensor was used on different samples such as serum, milk, honey and tablet. The serum samples were spiked with standard TC solution (1.0×10^{-4} μM, 1.0×10^{-2} μM), the honey and milk samples were spiked with standard TC solution (1.0×10^{-5} μM, 1.0×10^{-3} μM), and the tablet samples were spiked with standard TC solution (1.0×10^{-6} μM, 1.0×10^{-4} μM). In this work, the spiking was performed after the pretreatment, and the samples were diluted 10 times with buffer before analysis. The recoveries for the spiked samples ranged from 95% to 104%, implying that the aptasensor had a good accuracy. The spiked TC solutions were lower than that of EU standard required in milk (1 μM), indicating that spiking performed was correct and relevant for TC expected amounts in the milks.

In Wang's work [91], the developed aptasensor was used on milk samples. The recoveries and RSDs obtained by the proposed method and a commercial ELISA method. The spiking was performed before the pretreatment, and the samples were diluted 40 times with buffer before analysis. The milk samples were spiked with standard TC and OTC solution (2.25 μM, 1.69 μM, and 1.12 μM, respectively). The recoveries of the proposed method and ELISA method for TC were 99.03–102.66% and 97.50–102.95% with RSDs in the range of 5.71–6.84% and 5.25–6.02%, the recoveries for OTC were 97.32–100.47% and 99.44–102.18% with RSDs of 5.63–6.05% and 4.87–6.21%. The results obtained from the two methods were coincident. The spiking performance in this work was correct. On another work [60], the milk samples were spiked with standard OTC solution (10 μM, 20 μM, and 30 μM). The spiking was performed before the pretreatment, and the samples were diluted 10 times with buffer before analysis. The spiked milk samples were also detected by HPLC for comparison. The amount found of proposed method and HPLC method for OTC were 10.9 μM, 18.9 μM, and 25.4 μM and 8.8 μM, 18.3 μM, and 25.2 μM. The recoveries of the proposed method and ELISA method for TC were 84.22–108.36% and 93.36–91.04% with RSDs in the range of 0.49–2.35% and 0.91–61.4%. It is obvious that the results from the developed aptasensor was in accordance with those from HPLC. Although the spiking was performed before the pretreatment, but the spiked TC solutions were higher than that of EU standard required in milk, indicating that spiking performance was incorrect in this work.

Except for mentioned literatures, most of the literatures lack of enough details [41,93,100,124,142]. Either not indicated the spiking was performed before or after pretreatment, or did not specify the dilution multiples. In conclusion, application of sensors for TCs in real samples must have a exact pretreatment to avoid the interference. The spiked standard TCs should at the levels that are relevant for TCs expected for amounts in the respective samples. And the sample dilution factor during pretreatment needs to be considered. To validate the results, we can use standard ELISA or HPLC method. The recoveries and RSDs can direct response the accuracy and reproducibility of the developed sensors.

6. Conclusion and future outlook

This review has given a brief overview about recent advances in promising sensor for TCs detection. Two main tetracycline antibiotics sensors, i.e. electrochemical and optical sensors, are shown in details. Optical detection methods including colorimetry, fluorescence, SPR, chemiluminescence, and SERS methods have been used to design TCs sensors. Colorimetric method is the fastest and simplest technique, which can recognize the presence of target only by unaided eye. But it is easy interfered by the background color of samples and suffers from relatively low sensitivity. To avoid this, one can choose fluorescence technique which is one of the most popular optical methods. Owing to its excellent characteristics, like easy detection procedure and high sensitivity, fluorescence method has been extensively used to TCs detection. However, the fluorophore has a short life time. Chemiluminescence technique is another attractive optical method. Compared with the fluorescence technique, chemiluminescence method has several advantages such as no requirement for an external light source, and longer life time than that of fluorophore ones. In addition, SPR method has been recommended for determination of TCs because it can detect the analyte by label-free and can realize real time detection at the same time with relative low LOD. Owing to the fast response of optical sensors, the test time of optical sensors are usually shorter than that of conventional methods. If there need to be detected at very high sensitivity, more accurate and sensitive techniques are required. On this occasion, electrochemical methods, such as voltammetric, impedimetric, and amperometric are suitable choices. Among the three electrochemical methods, voltammetry is the

Table 4
Compare detection methods for different applications in the area of quantitative detection of tetracycline.

Sensors type	Advantages	Shortcomings
Optical		
Colorimetric	Visual detection; Quick detection; Simple apparatus	Low sensitivity; Easy influenced by external environment; Interference from the background color of sample;
Fluorescent	Convenient operation; Easy automation	Short life time of fluorophore
SPR	Label-free; Real time detection	High cost of instrument
CL	Wide dynamic range; Low cost; Simple operation;	No real-time detection Labeling required
SERS	Simplicity; Rapidity; High sensitivity	Poor stability of substrates
Electrochemical		
Voltammetric	Easy detection; Method diversification	Poor stability of electrode
Impedimetric	Rapidity; Label-free detection; High sensitivity	Complicated process for modeling the electrode
Amperometric	High sensitivity; Automation; Miniaturisation	Labeling of the analyte to increase the electrochemical reaction at the electrode
Others		
PEC	Simple apparatus; Easy miniaturization; Fast response; Reduced background signal	Instability; High demand of flexible substrates
ECL	Low cost; High sensitivity	Easy influenced by external environment

SPR: surface Plasmon resonance; CL: chemiluminescence; SERS: surface-enhanced Raman scattering; PEC: photoelectrochemical; ECL: electrochemiluminescence.

most common used technique, because of its easy detection, excellent sensitivity and selectivity. Meanwhile voltammetry has a lot of alternative techniques, such as DPV, and CV, etc.. Impedimetric method include EIS technique and it has more widely linear range and lower LOD compared with DPV technique. In general, electrochemical methods equip with high sensitivity and wide detection range, but it suffered from poor repeatability, and the electrodes are sensitive to external environment so they need intricate sample pretreatment. The test time of electrochemical sensors are longer than that of optical sensors but shorter than that of conventional methods. Except for two main TCs sensors, i.e. electrochemical and optical sensors, we also introduced other TCs sensors, such as electrochemiluminescence and photoelectrochemical methods in details. Electrochemiluminescence method is a well-known high sensitivity detection assay which combines the sensitivity of chemiluminescence with the advantages of electrochemistry. Photoelectrochemical method has been paid a growing attention because it reveals greater performance than traditional electrochemical and optical sensors. Owing to photoelectrochemical method combines the advantages of traditional electrochemical and optical sensors, it has some significant advantages, such as easy miniaturization, simple apparatus, fast response, ultrahigh sensitivity, and reduced background signal. Therefore, each kind of TCs sensors possesses its own disadvantages and advantages (see Table 4).

Despite some advantages of these sensors compared with conventional detection methods, there are still some challenges for further application of these advances sensors. For example, sensitivity and selectivity in some designed methods depend on measuring environment such as temperature, pH, ionic strength, etc.. On the other hand, selection of receptor elements (such as aptamer, MIPs, functional molecules, etc.) and signal transducer (nanomaterial, substrate, etc.) is time-consuming and difficult process. Therefore, an important challenge in antibiotics sensors is the practical application, i.e. on-site analysis of targets in real world, complex environments. That is, the final goal of all the sensing devices should face to the end user. Unfortunately, till now the innovation has been restricted to the laboratory scale and it has not reached to end user who badly needs a smart quick sensing reliable tool. Therefore, an effective technology, enabling rapid production of large amounts of antibiotic sensors with high-quality specifications and relatively low cost, are still highly desired. Such a technique is the prerequisite for the successful commercial application of any sensing devices. Future efforts should be made on developing multifunctional and environmentally friendly nanomaterials and making the antibiotic sensors more robust. What's more, for further application in real samples, the recognition elements including bio-recognition and chemical-recognition elements, and signal transducer should also be improved, because of the higher tolerance to the more complex and harsh natural environmental conditions. Nevertheless, we expect the research in TCs biosensors and chemosensors will still continuous hot. We also hope that sensors can be widely used in antibiotic detection or even drug detection and eventually become effectively routine analysis tools that could meet various challenges.

Acknowledgement

This study was financially Supported by the Program for the National Natural Science Foundation of China (51879101, 51579098, 51779090, 51709101, 51408206, 51521006), Science and Technology Plan Project of Hunan Province (2018SK20410, 2017SK2243, 2016RS3026), the National Program for Support of Top−Notch Young Professionals of China (2014), the Program for Changjiang Scholars and Innovative Research Team in University (IRT-13R17), and the Fundamental Research Funds for the Central Universities (531109200027, 531107050978, 531107051080).

References

[1] C. Zhang, C. Lai, G. Zeng, D. Huang, C. Yang, Y. Wang, Y. Zhou, M. Cheng, Water Res. 95 (2016) 103.
[2] D. Huang, X. Wang, C. Zhang, G. Zeng, Z. Peng, J. Zhou, M. Cheng, R. Wang, Z. Hu, X. Qin, Chemosphere 186 (2017) 414.
[3] H. Yi, D. Huang, L. Qin, G. Zeng, C. Lai, M. Cheng, S. Ye, B. Song, X. Ren, X. Guo, Appl. Catal. B Environ. 239 (2018) 408.
[4] S. Wang, W. Yong, J. Liu, L. Zhang, Q. Chen, Y. Dong, Biosens. Bioelectron. 57 (2014) 192.
[5] B. Li, C. Lai, G. Zeng, L. Qin, H. Yi, D. Huang, C. Zhou, X. Liu, M. Cheng, P. Xu, C. Zhang, F. Huang, S. Liu, ACS Appl. Mater. Interfaces 10 (2018) 18824.
[6] F. Conzuelo, M. Gamella, S. Campuzano, A.J. Reviejo, J.M. Pingarron, Anal. Chim. Acta 737 (2012) 29.
[7] Q. Zhou, Y. Zhang, N. Wang, L. Zhu, H. Tang, Food Contr. 46 (2014) 324.
[8] R.T. Kushikawa, M.R. Silva, A.C.D. Angelo, M.F.S. Teixeira, Sensor. Actuators B Chem. 228 (2016) 207.
[9] D. Huang, W. Xue, G. Zeng, J. Wan, G. Chen, C. Huang, C. Zhang, M. Cheng, P. Xu, Water Res. 106 (2016) 15.
[10] J. Xue, J. Liu, C. Wang, Y. Tian, N. Zhou, Anal. Meth. 8 (2016) 1981.
[11] X. Gong, D. Huang, Y. Liu, Z. Peng, G. Zeng, P. Xu, M. Cheng, R. Wang, J. Wan, Crit. Rev. Biotechnol. (2017) 1.
[12] D. Huang, X. Guo, Z. Peng, G. Zeng, P. Xu, X. Gong, R. Deng, W. Xue, R. Wang, H. Yi, Crit. Rev. Biotechnol. (2017) 1.
[13] X. Gong, D. Huang, Y. Liu, G. Zeng, R. Wang, J. Wei, C. Huang, P. Xu, J. Wan, C. Zhang, Bioresour. Technol. 253 (2018) 64.
[14] A. Wong, M. Scontri, E.M. Materon, M.R.V. Lanza, M.D.P.T. Sotomayor, J. Electroanal. Chem. 757 (2015) 250.
[15] D. Huang, L. Liu, G. Zeng, P. Xu, C. Huang, L. Deng, R. Wang, J. Wan, Chemosphere 174 (2017) 545.
[16] H.A.T. Regulation, Offic. J. L 224 (1990) 0001.

[17] R.W. Fedeniuk, S. Ramamurthi, A.R. McCurdy, J. Chromatogr. B Biomed. Sci. Appl. 677 (1996) 291.
[18] X. Gong, D. Huang, Y. Liu, G. Zeng, R. Wang, J. Wan, C. Zhang, M. Cheng, X. Qin, W. Xue, Environ. Sci. Technol. 51 (2017) 11308.
[19] W. Xue, D. Huang, G. Zeng, J. Wan, C. Zhang, R. Xu, M. Cheng, R. Deng, J. Hazard. Mater. 341 (2018) 381.
[20] J. Li, L. Chen, X. Wang, H. Jin, L. Ding, K. Zhang, H. Zhang, Talanta 75 (2008) 1245.
[21] W. Naidong, S. Hua, E. Roets, J. Hoogmartens, J. Pharmaceut. Biomed. Anal. 33 (2003) 85.
[22] P. Kowalski, J. Pharm. Biomed. Anal. 47 (2008) 487.
[23] J. Tong, Q. Rao, K. Zhu, Z. Jiang, S. Ding, J. Sep. Sci. 32 (2009) 4254.
[24] D.S. Aga, R. Goldfish, P. Kulshrestha, Analyst 128 (2003) 658.
[25] L. Lan, Y. Yao, J. Ping, Y. Ying, Biosens. Bioelectron. 91 (2017) 504.
[26] V. Gaudin, Biosens. Bioelectron. 90 (2017) 363.
[27] Y. Li, J. Xu, C. Sun, RSC Adv. 5 (2015) 1125.
[28] C. Lai, G.-M. Zeng, D.-L. Huang, M.-H. Zhao, M. Chen, Z. Wei, C. Huang, P. Xu, N.-J. Li, X. Li, Anal. Meth. 6 (2014) 312.
[29] Y. Zhou, L. Tang, G. Zeng, C. Zhang, X. Xie, Y. Liu, J. Wang, J. Tang, Y. Zhang, Y. Deng, Talanta 146 (2016) 641.
[30] D. Wu, D. Du, Y. Lin, Trac. Trends Anal. Chem. 83 (2016) 95.
[31] W. Tu, Z. Wang, Z. Dai, Trac. Trends Anal. Chem. 105 (2018) 470.
[32] A. Waheed, M. Mansha, N. Ullah, Trac. Trends Anal. Chem. 105 (2018) 37.
[33] X. Yan, H. Li, X. Su, Trac. Trends Anal. Chem. 103 (2018) 1.
[34] S.-Y. Wang, C.-F. Wang, Y.-K. Lv, S.-G. Shen, Trac. Trends Anal. Chem. 106 (2018) 53.
[35] Y. Zhou, L. Tang, G. Zeng, J. Chen, J. Wang, C. Fan, G. Yang, Y. Zhang, X. Xie, Biosens. Bioelectron. 65 (2015) 382.
[36] Y. Zhou, L. Tang, G. Zeng, C. Zhang, Y. Zhang, X. Xie, Sensor. Actuators B Chem. 223 (2016) 280.
[37] L. Qin, G. Zeng, C. Lai, D. Huang, P. Xu, C. Zhang, M. Cheng, X. Liu, S. Liu, B. Li, Coord. Chem. Rev. 359 (2018) 1.
[38] M. Ramezani, N. Mohammad Danesh, P. Lavaee, K. Abnous, S. Mohammad Taghdisi, Biosens. Bioelectron. 70 (2015) 181.
[39] Y.S. Kim, J.H. Kim, I.A. Kim, S.J. Lee, J. Jurng, M.B. Gu, Biosens. Bioelectron. 26 (2010) 1644.
[40] B. Tan, H. Zhao, L. Du, X. Gan, X. Quan, Biosens. Bioelectron. 83 (2016) 267.
[41] F. Yuan, H. Zhao, Z. Zhang, L. Gao, J. Xu, X. Quan, RSC Adv. 5 (2015) 58895.
[42] M. Lin, H.Y. Zou, T. Yang, Z.X. Liu, H. Liu, C.Z. Huang, Nanoscale 8 (2016) 2999.
[43] Y. Wang, Y. Sun, H. Dai, P. Ni, S. Jiang, W. Lu, Z. Li, Z. Li, Sensor. Actuators B Chem. 236 (2016) 621.
[44] X. An, S. Zhuo, P. Zhang, C. Zhu, RSC Adv. 5 (2015) 19853.
[45] Y. Feng, D. Zhong, H. Miao, X. Yang, Talanta 140 (2015) 128.
[46] L. Zhang, L. Chen, ACS Appl. Mater. Interfaces 8 (2016) 16248.
[47] E. Song, M. Yu, Y. Wang, W. Hu, D. Cheng, M.T. Swihart, Y. Song, Biosens. Bioelectron. 72 (2015) 320.
[48] R.Y. Robati, A. Arab, M. Ramezani, F.A. Langroodi, K. Abnous, S.M. Taghdisi, Biosens. Bioelectron. 82 (2016) 162.
[49] C. Feng, S. Dai, L. Wang, Biosens. Bioelectron. 59 (2014) 64.
[50] Y. Song, W. Wei, X. Qu, Adv. Mater. 23 (2011) 4215.
[51] C. Lai, L. Qin, G. Zeng, Y. Liu, D. Huang, C. Zhang, P. Xu, M. Cheng, X. Qin, M. Wang, RSC Adv. 6 (2016) 3259.
[52] C. Lai, X. Liu, L. Qin, C. Zhang, G. Zeng, D. Huang, M. Cheng, P. Xu, H. Yi, D. Huang, Microchim. Acta 184 (2017) 2097.
[53] L. Qin, G. Zeng, C. Lai, D. Huang, C. Zhang, P. Xu, T. Hu, X. Liu, M. Cheng, Y. Liu, Sensor. Actuators B Chem. 243 (2017) 946.
[54] C. Zhang, G. Zeng, D. Huang, C. Lai, C. Huang, N. Li, P. Xu, M. Cheng, Y. Zhou, W. Tang, RSC Adv. 4 (2014) 55511.
[55] S. Tombelli, M. Minunni, M. Mascini, Biosens. Bioelectron. 20 (2005) 2424.
[56] R. Liu, C. Wang, J. Hu, Y. Su, Y. Lv, Trac. Trends Anal. Chem. 105 (2018) 436.
[57] S. Wang, S. Gao, S. Sun, Y. Yang, Y. Zhang, J. Liu, Y. Dong, H. Su, T. Tan, RSC Adv. 6 (2016) 45645.
[58] Y.S. Kwon, N.H. Ahmad Raston, M.B. Gu, Chem. Commun. (Camb) 50 (2014) 40.
[59] L. He, Y. Luo, W. Zhi, P. Zhou, Food Anal. Meth. 6 (2013) 1704.
[60] R. Su, J. Xu, Y. Luo, Y. Li, X. Liu, J. Bie, C. Sun, Mater. Lett. 180 (2016) 31.
[61] L. Shen, J. Chen, N. Li, P. He, Z. Li, Anal. Chim. Acta 839 (2014) 83.
[62] J. Li, S. Fan, Z. Li, Y. Xie, R. Wang, B. Ge, J. Wu, R. Wang, Optic. Spectrosc. 117 (2014) 250.
[63] D. Huang, C. Hu, G. Zeng, M. Cheng, P. Xu, X. Gong, R. Wang, W. Xue, Sci. Total Environ. 574 (2017) 1599.
[64] M. Cheng, G. Zeng, D. Huang, C. Lai, P. Xu, C. Zhang, Y. Liu, Chem. Eng. J. 284 (2016) 582.
[65] J. Li, D. Yim, W.-D. Jang, J. Yoon, Chem. Soc. Rev. 46 (2017) 2437.
[66] H. Yi, G. Zeng, C. Lai, D. Huang, L. Tang, J. Gong, M. Chen, P. Xu, H. Wang, M. Cheng, Chem. Eng. J. 330 (2017) 134.
[67] A. Karimzadeh, M. Hasanzadeh, N. Shadjou, M.d.l. Guardia, Trac. Trends Anal. Chem. 105 (2018) 484.
[68] V. Kumar, P. Kumar, A. Pournara, K. Vellingiri, K.-H. Kim, Trac. Trends Anal. Chem. 106 (2018) 84.
[69] C. Gao, Z. Liu, J. Chen, Z. Yan, Luminescence 28 (2013) 378.
[70] X. Zhou, C. Lai, D. Huang, G. Zeng, L. Chen, L. Qin, P. Xu, M. Cheng, C. Huang, C. Zhang, J. Hazard. Mater. 346 (2018) 113.
[71] C. Lai, M.-M. Wang, G.-M. Zeng, Y.-G. Liu, D.-L. Huang, C. Zhang, R.-Z. Wang, P. Xu, M. Cheng, C. Huang, H.-P. Wu, L. Qin, Appl. Surf. Sci. 390 (2016) 368.
[72] D.-L. Huang, R.-Z. Wang, Y.-G. Liu, G.-M. Zeng, C. Lai, P. Xu, B.-A. Lu, J.-J. Xu, C. Wang, C. Huang, Environ. Sci. Pollut. Res. 22 (2015) 963.
[73] X. Zhou, C. Lai, D. Huang, G. Zeng, L. Chen, L. Qin, P. Xu, M. Cheng, C. Huang, C. Zhang, J. Hazard. Mater. 346 (2018) 113.
[74] M.R. Chao, C.W. Hu, J.L. Chen, Biosens. Bioelectron. 61 (2014) 471.
[75] L. Lin, Y. Luo, P. Tsai, J. Wang, X. Chen, Trac. Trends Anal. Chem. 103 (2018) 87.
[76] Y. Wang, A. Hu, J. Mater. Chem. C 2 (2014) 6921.
[77] S.Y. Lim, W. Shen, Z. Gao, Chem. Soc. Rev. 44 (2015) 362.
[78] Z. Peng, X. Han, S. Li, A.O. Al-Youbi, A.S. Bashammakh, M.S. El-Shahawi, R.M. Leblanc, Coord. Chem. Rev. 343 (2017) 256.
[79] J. Hou, J. Yan, Q. Zhao, Y. Li, H. Ding, L. Ding, Nanoscale 5 (2013) 9558.
[80] J. Hou, H. Li, L. Wang, P. Zhang, T. Zhou, H. Ding, L. Ding, Talanta 146 (2016) 34.
[81] A.N. Brown, K. Smith, T.A. Samuels, J. Lu, S.O. Obare, M.E. Scott, Appl. Environ. Microbiol. 78 (2012) 2768.
[82] F. Fernández, K. Hegnerová, M. Piliarik, F. Sanchez-Baeza, J. Homola, M.-P. Marco, Biosens. Bioelectron. 26 (2010) 1231.
[83] N. de-los-Santos-Álvarez, M.J. Lobo-Castañón, A.J. Miranda-Ordieres, P. Tuñón-Blanco, Biosens. Bioelectron. 24 (2009) 2547.
[84] S. Zeng, D. Baillargeat, H.-P. Ho, K.-T. Yong, Chem. Soc. Rev. 43 (2014) 3426.
[85] R. Verma, B.D. Gupta, Analyst 138 (2013) 7254.
[86] M. Amjadi, J.L. Manzoori, F. Pakpoor, J. Anal. Chem. 71 (2016) 253.
[87] S. Kim, H.J. Lee, Anal. Chem. 89 (2017) 6624.
[88] W. Miao, Chem. Rev. 108 (2008) 2506.
[89] S. Cho, L. Park, R. Chong, Y.T. Kim, J.H. Lee, Biosens. Bioelectron. 52 (2014) 310.
[90] J. Yakovleva, R. Davidsson, M. Bengtsson, T. Laurell, J. Emnéus, Biosens. Bioelectron. 19 (2003) 21.
[91] L. Hao, H. Gu, N. Duan, S. Wu, Z. Wang, Anal. Meth. 8 (2016) 7929.
[92] W. Zeng, C. Zhu, H. Liu, J. Liu, H. Cai, X. Cheng, L. Wei, J. Lumin. 186 (2017) 158.
[93] H. Li, Q. Chen, M. Mehedi Hassan, X. Chen, Q. Ouyang, Z. Guo, J. Zhao, Biosens. Bioelectron. 92 (2017) 192.
[94] J. Zhao, P. Liu, H. Yuan, Y. Peng, Q. Hong, M. Liu, J. Spectrosc. 2016 (2016) 1.
[95] J. Kneipp, H. Kneipp, K. Kneipp, Chem. Soc. Rev. 37 (2008) 1052.
[96] D. Jin, Y. Bai, H. Chen, S. Liu, N. Chen, J. Huang, S. Huang, Z. Chen, Anal. Meth. 7 (2015) 1307.
[97] R. Li, H. Zhang, Q.W. Chen, N. Yan, H. Wang, Analyst 136 (2011) 2527.
[98] F. Meng, X. Ma, N. Duan, S. Wu, Y. Xia, Z. Wang, B. Xu, Talanta 165 (2017) 412.
[99] X. Li, H. Ma, M. Deng, A. Iqbal, X. Liu, B. Li, W. Liu, J. Li, W. Qin, J. Mater. Chem. C 5 (2017) 2149.
[100] F. Qu, Z. Sun, D. Liu, X. Zhao, J. You, Microchim. Acta 183 (2016) 2547.
[101] A. Wang, Y. Bai, H. Gao, S. Wang, Anal. Meth. 7 (2015) 6842.
[102] X. Li, C. Li, L. Chen, New J. Chem. 39 (2015) 9976.
[103] H. Tan, C. Ma, Y. Song, F. Xu, S. Chen, L. Wang, Biosens. Bioelectron. 50 (2013) 447.
[104] S.H. Jalalian, S.M. Taghdisi, N.M. Danesh, H. Bakhtiari, P. Lavaee, M. Ramezani, K. Abnous, Anal. Meth. 7 (2015) 2523.
[105] X. Yang, S. Zhu, Y. Dou, Y. Zhuo, Y. Luo, Y. Feng, Talanta 122 (2014) 36.
[106] H. Tan, Y. Chen, Sensor. Actuators B Chem. 173 (2012) 262.
[107] G. Zeng, C. Zhang, D. Huang, C. Lai, L. Tang, Y. Zhou, P. Xu, H. Wang, L. Qin, M. Cheng, Biosens. Bioelectron. 90 (2017) 542.
[108] C. Zhang, C. Lai, G. Zeng, D. Huang, L. Tang, C. Yang, Y. Zhou, L. Qin, M. Cheng, Biosens. Bioelectron. 81 (2016) 61.
[109] S.M. Taghdisi, N.M. Danesh, M. Ramezani, K. Abnous, Biosens. Bioelectron. 85 (2016) 509.
[110] G. Kaur, M. Tomar, V. Gupta, Biosens. Bioelectron. 80 (2016) 294.
[111] L. Zhou, D.-J. Li, L. Gai, J.-P. Wang, Y.-B. Li, Sensor. Actuators B Chem. 162 (2012) 201.
[112] A. Benvidi, N. Rajabzadeh, M. Mazloum-Ardakani, M.M. Heidari, A. Mulchandani, Biosens. Bioelectron. 58 (2014) 145.
[113] A. Benvidi, N. Rajabzadeh, H.M. Zahedi, M. Mazloum-Ardakani, M.M. Heidari, L. Hosseinzadeh, Talanta 137 (2015) 80.
[114] X.R. Cheng, B.Y. Hau, T. Endo, K. Kerman, Biosens. Bioelectron. 53 (2014) 513.
[115] S. Jahanbani, A. Benvidi, Biosens. Bioelectron. 85 (2016) 553.
[116] X. Liu, S. Zheng, Y. Hu, Z. Li, F. Luo, Z. He, Food Anal. Meth. 9 (2016) 2972.
[117] A. Benvidi, M.D. Tezerjani, S.M. Moshtaghiun, M. Mazloum-Ardakani, Microchim. Acta 183 (2016) 1797.
[118] T.H. Le, V.P. Pham, T.H. La, T.B. Phan, Q.H. Le, Adv. Nat. Sci. Nanosci. Nanotechnol. 7 (2016) 015008.
[119] D. Chen, D. Yao, C. Xie, D. Liu, Food Contr. 42 (2014) 109.
[120] Q.-C. Xu, Q.-Q. Zhang, X. Sun, Y.-M. Guo, X.-Y. Wang, RSC Adv. 6 (2016) 17328.
[121] Y. Guo, X. Wang, X. Sun, Int. J. Electrochem. Sci. 10 (2015) 3668.
[122] F. Conzuelo, S. Campuzano, M. Gamella, D.G. Pinacho, A.J. Reviejo, M.P. Marco, J.M. Pingarron, Biosens. Bioelectron. 50 (2013) 100.
[123] J. Ghodsi, A.A. Rafati, Y. Shoja, Sensor. Actuators B Chem. 224 (2016) 692.
[124] X. Zhan, G. Hu, T. Wagberg, S. Zhan, H. Xu, P. Zhou, Microchim. Acta 183 (2015) 723.
[125] Y. Guo, G. Shen, X. Sun, X. Wang, IEEE Sensor. J. 15 (2015) 1951.
[126] H. Wang, H. Zhao, X. Quan, S. Chen, Electroanalysis 23 (2011) 1863.
[127] X. Sun, G. Shen, Y. Guo, X. Wang, Nano Micro Lett. 6 (2014).
[128] M.B. Gholivand, H. Khani, Electroanalysis 25 (2013) 461.

[129] Y.J. Kim, Y.S. Kim, J.H. Niazi, M.B. Gu, Bioproc. Biosyst. Eng. 33 (2010) 31.
[130] Z. Liu, W. Qi, G. Xu, Chem. Soc. Rev. 44 (2015) 3117.
[131] Z. Guo, P. Gai, Anal. Chim. Acta 688 (2011) 197.
[132] X. Chen, L. Zhao, X. Tian, S. Lian, Z. Huang, X. Chen, Talanta 129 (2014) 26.
[133] B. Deng, Q. Xu, H. Lu, L. Ye, Y. Wang, Food Chem. 134 (2012) 2350.
[134] W.-W. Zhao, J.-J. Xu, H.-Y. Chen, Chem. Rev. 114 (2014) 7421.
[135] T. Hisatomi, J. Kubota, K. Domen, Chem. Soc. Rev. 43 (2014) 7520.
[136] K. Yan, Y. Liu, Y. Yang, J. Zhang, Anal. Chem. 87 (2015) 12215.
[137] H. Li, J. Li, Y. Qiao, H. Fang, D. Fan, W. Wang, Sensor. Actuators B Chem. 243 (2017) 1027.
[138] Y. Liu, K. Yan, J. Zhang, ACS Appl. Mater. Interfaces 8 (2016) 28255.
[139] Y. Li, J. Tian, T. Yuan, P. Wang, J. Lu, Sensor. Actuators B Chem. 240 (2017) 785.
[140] C. Zhou, C. Lai, D. Huang, G. Zeng, C. Zhang, M. Cheng, L. Hu, J. Wan, W. Xiong, M. Wen, Appl. Catal. B Environ. 220 (2018) 202.
[141] M. Bougrini, A. Florea, C. Cristea, R. Sandulescu, F. Vocanson, A. Errachid, B. Bouchikhi, N. El Bari, N. Jaffrezic-Renault, Food Contr. 59 (2016) 424.
[142] Y. Chen, Q. Chen, M. Han, J. Liu, P. Zhao, L. He, Y. Zhang, Y. Niu, W. Yang, L. Zhang, Biosens. Bioelectron. 79 (2016) 430.